

CURE STUDIES OF NETWORK-FORMING POLYURETHANES

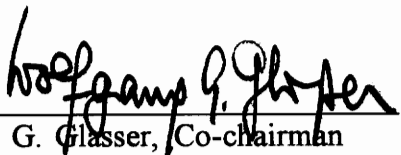
by

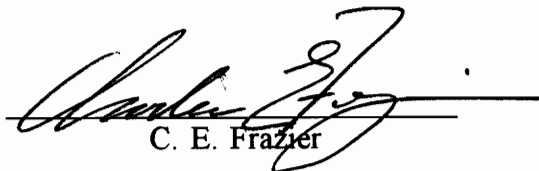
Ackah Toffey

Thesis submitted to the Faculty of
Virginia Polytechnic Institute and State University
in partial fulfillment of the requirements for
the degree of
Master of Science
in
Forest Products

APPROVED:


R. L. Youngs, Co-chairman


W. G. Glasser, Co-chairman


C. E. Frazier

October 1993

Blacksburg, Virginia

C.2

LD
5655
V855
1993
T633
C.2

CURE STUDIES OF NETWORK-FORMING POLYURETHANES

by

Ackah Toffey

R. L. Youngs, Co-chairman

W. G. Glasser, Co-chairman

Forest Products

(ABSTRACT)

The polyhydroxy character of lignocellulosics and their natural abundance make them good candidates for the manufacture of polyurethanes.

The cure characteristics of hydroxypropyl-cellulose and hydroxypropyl lignin (HPC and HPL, respectively) with polymeric methylene diphenyl diisocyanate (MDI) was studied via dynamic mechanical thermal analysis (DMTA).

HPC/MDI and HPL/MDI resins flow at 30°C and proceed to cure at 50°C. The latter has excellent thermal stability over the former. Crosslinking of HPL and HPC with MDI follow an nth order kinetics, with an order of reaction of 2 and an apparent activation energy in the range of 12.9 kcal/mol - 14.7 kcal/mol.

The rate of cure with time is higher in HPL-based polymers than HPC-based ones at the initial stage of cure; the difference vanishes at later stages. This demonstrates that the hydroxyl groups in HPC are less accessible to the NCO groups, and that cure rate might be dependent on diffusion limitations at later stages.

Degree of cure, under all cure schedules, follows a parallel trend, and has to do with the fact that the hydroxyl groups of HPC are less accessible to isocyanate. Both HPL and HPC react with MDI at a reduced rate in comparison to a synthetic polyol: caprolactone triol.

Time-glass transition temperature superposition was used to calculate times to vitrification of the HPL-based polymers, and is presented in a TTT cure diagram. This bio-based polymer displays the s-shaped vitrification pattern characteristics of thermosets. A similar approach did not work with HPC-based polymers. HPC- and HPL-based polymers did not display damping transitions, in isothermal cure, typical of gelation and vitrification. As the isocyanate to hydroxyl ratio (NCO:OH) increased, the glass transition temperature of the polymers increased, and the transition amplitude and width decreased and increased, respectively.

In practical terms, this study illustrates that it is advantageous to use

- a) to use high isocyanate to hydroxyl ratios in order to produce polyurethanes which retain desirable damping behavior over a wider range of temperature.
- b) to use HPC/MDI resins in those situations where retention of stiffness at temperatures below 230° is required.
- c) to use HPL where rapid cure is desired.

The study also reveals that the relative reactivity of water, HPL and HPC with isocyanate takes the form water > HPL > HPC.

ACKNOWLEDGEMENTS

The author expresses his gratitude to his co-advisors, Professors Robert L. Youngs and Wolfgang G. Glasser, for their encouragement and support in pursuing my graduate program, and their guidance in thesis research.

Thanks are due Professor Charles E. Frazier for many valuable discussions. I am very grateful to Dr. Gamini Saramanayaki for his intense involvement in this work. His assistance and guidance were indispensable in the course of completing this work.

The assistance of James Sealey and Paul Vail in instrumental analysis is also very much appreciated. The author expresses his gratitude to Professor Geza Ifju for his assistance in getting him enrolled at Virginia Tech.

Finally, the author expresses his thanks to his dear wife, Sophia, for her moral and personal support.

TABLE OF CONTENTS

	Page
ABSTRACT	ii
ACKNOWLEDGEMENTS	iv
TABLE OF CONTENTS	v
LIST OF FIGURES	viii
LIST OF TABLES	xii
1.0 INTRODUCTION	1
2.0 LITERATURE REVIEW	4
2.1 NETWORK FORMATION AND THERMOSET CURE	4
2.1.1 Theory of Thermosetting Polymers	4
2.1.2 Network-forming Polyurethanes	6
2.1.3 Parameters Influencing Network Formation	7
2.2 CURE CHARACTERIZATION TECHNIQUES	14
2.2.1 Chemical Methods	16
2.2.2 Physical Methods	16
2.3 TIME-TEMPERATURE-TRANSFORMATION CURE DIAGRAMS .	30
2.3.1 A Schematic TTT Cure Diagram	31
2.3.2 Experimental Aspect of the TTT Cure Diagram and Data Interpretation	34
2.3.3 Time-temperature shift of T_g versus time	39

3.0	MATERIALS AND METHODS	43
3.1	MATERIALS	43
3.1.1	Isocyanates	43
3.1.2	Polyols	43
3.2	METHODS	45
3.2.1	Resin Preparation	45
3.2.2	Samples Preparation	45
3.2.3	Product Analysis and Testing	47
4.0	RESULTS AND DISCUSSION	49
4.1	MODEL CONSIDERATION	49
4.2	DYNAMIC TEMPERATURE SCAN OF RESINS	51
4.3	ISOTHERMAL CURE OF RESINS	56
4.4	KINETICS OF HPC AND HPL CROSSLINKING WITH ISOCYANATE	66
4.5	GLASS TRANSITION TEMPERATURE OF PARTIALLY CURED POLYURETHANES	78
4.6	CONSTRUCTION OF VITRIFICATION CURVE IN A TTT CURE DIAGRAM	84
4.7	FRACTIONAL CURE VERSUS TIME SHIFTING	84
4.8	EFFECT OF RESIN STOICHIOMETRY ON NETWORK FORMATION	91

5.0 CONCLUSIONS	98
VITA	101
REFERENCES	102

LIST OF FIGURES

	Page
Figure 1	A schematic diagram of T_g vs conversion at vitrification for reactants differing in functionality 9
Figure 2	A DMTA spectrum depicting the effect of increasing molecular weight on the T_g of polyurethanes from lignin fractions . . . 11
Figure 3	DMTA spectra of an epoxy resin depicting the variation of vitrification and gelation with cure temperature 15
Figure 4	A hypothetical DMTA relative modulus profile as a function of temperature during cure 26
Figure 5	An isothermal cure profile of an epoxy resin 29
Figure 6	A schematic TTT cure diagram for a thermosetting polymer showing the different states encountered during cure 32
Figure 7	Time to gelation and time to vitrification vs temperature of isothermal cure 37
Figure 8	Methods for determining times to gelation and vitrification 38
Figure 9	A temperature scan profile of HPL-based resin 52
Figure 10	A temperature scan profile of HPC-based resin 53
Figure 11 a&b	Isothermal cure profile of HPC-based resins 57

Figure 12	An illustration of nonconformity to the criterion of using E' and E'' crossover as gelation in the HPC-based polyurethanes . . .	59
Figure 13	Glass transition temperature of HPC- and HPL-based polyurethanes versus cure temperature	60
Figure 14	Characteristic transitions displayed by HPC- and HPL-based polyurethanes	62
Figure 15	Comparison of T_g of HPC-based polyurethanes for various isothermal cure times at T_c of 90°C	64
Figure 16 a&b	Arrhenius plots of $\ln k$ versus reciprocal temperature	67
Figure 17 a&b	Rate of cure and degree of cure in HPC and HPL-based resins	70
Figure 18	Rate of cure with temperature in HPC and HPL-based resins	72
Figure 19	Rate expression versus time for the determination of rate constants at various cure temperatures	75
Figure 20	Arrhenius plot of rate constant versus temperature for activation energy determination	76
Figure 21	Evaluation of model equation and order of reaction of HPC-based polyurethanes	77
Figure 22	T_g versus time at various cure temperatures for HPL-based polymers	80

Figure 23	T_g versus time master curve at an arbitrarily chosen reference temperature 80°C	82
Figure 24	Arrhenius plot of shift factors, $A(T)$ used in constructing the master curves at 80°C versus reciprocal temperature	83
Figure 25	Calculated isothermal TTT diagram showing vitrification curve of HPL-based polyurethanes	85
Figure 26	Fractional cure of HPC-based polyurethanes versus time at various temperatures	87
Figure 27	Fractional cure master curve at an arbitrarily chosen reference cure temperature, 120°C	88
Figure 28	Arrhenius plot of shift factors $A(T)$, used in constructing the fractional cure master curve at 120°C versus reciprocal temperature	89
Figure 29	Iso-fractional cure profile of HPC-based polymers	90
Figure 30	The variation of T_g and its activation energy derived from an Arrhenius plot of \ln frequency versus T_g , with resin stoichiometry	92
Figure 31	DMTA spectra of HPL-based polymers showing the effect of frequency on T_g	93
Figure 32	Arrhenius plot of (frequency) versus T_g for the determination of the activation energy of T_g of HPL-based polyurethanes at various resin stoichiometries	94

Figure 33

Change of damping characteristics in HPL-based polymers with
NCO:OH 97

LIST OF TABLES

	Page
Table 1	Properties of polyurethane components 44
Table 2	Formulation of polyurethanes 46
Table 3	Temperature of vitrification, gelation, and the glass transition temperature of the uncured resins 54
Table 4	Comparison of activation energy of polyurethane cure 68
Table 5	Isothermal and dynamic kinetic cure parameters 73
Table 6	Shift factors for T_g shifting 81
Table 7	Activation energy of T_g at various resin stoichiometries 95

CHAPTER 1

1.0 INTRODUCTION

Isocyanate adhesives have received considerable attention in the forest products industry, particularly the wood-based composite industry, in recent years. Methylene diphenyl diisocyanate (MDI) is currently used as a binder for composite wood panels,⁴⁷ and its application is expected to be on the rise as the industry seeks to find viable alternatives to replace formaldehyde-emitting adhesives. There are opposing views about the mechanism of isocyanate cure during wood bonding. One school of thought believes that the predominant reaction is that between isocyanate and hydroxyl groups of wood components to form urethane linkages. The other, by contrast, considers the reaction of isocyanate with moisture in wood to form urea linkages as the predominant one.

The larger benefit of MDI and other isocyanates may, however, ultimately come from their capability to crosslink linear/non-cyclic and other polymers. The polyurethanes, which have been engineered to penetrate various materials communities (adhesives, coatings, foams, elastomers, etc.) owe their existence to the ability of isocyanates to crosslink hydroxyl-containing compounds (polyols). The markets for polyurethanes, worldwide, have continuously grown over the past ten years. Today, more than 80% of our upholstered furniture, and automobiles are

cushioned with polyurethanes, and are expected to make inroads into other applications. Polyurethanes consume large amounts of oil-derived polyols. These can be manufactured from renewable resources cost-effectively, and should support or sustain the chemical industry.

The polyhydroxy character of lignocellulosics and their natural abundance should make them good candidates for polyurethane utilization research.

Glasser and co-workers have pioneered the utilization of lignocellulosics as polyols for polyurethanes.^{22,23,37,38} Their studies have been devoted to characterizing lignin and cellulose-based polyurethanes, in terms of the following: effect of molar substitution, network density, added soft segment, lignin type, diisocyanate type, and molecular weight. However, there has been no reported study on the cure kinetics of these polymer systems. Such a study could be of great practical interest since the ultimate properties of a polymer depend in large part on the network structure that is formed during cure, the latter being dependent on reaction kinetics, and other formulation variables.

The systematic and elaborate study of cure kinetics, network formation, viscoelastic and mechanical properties of the epoxy resins has led to a better understanding of the behavior of these polymers, and made them the preferred choice for a wide array of applications, such as aerospace and coating applications. Much of their behavior during cure has been studied in terms of the time-temperature-transformation (TTT) cure diagrams proposed by Gillham.¹⁵

To propel lignocellulosic-based polyurethanes to industrial acceptance and/or level of the epoxy polymers, it is critical to investigate the cure kinetics, network formation, and viscoelastic properties, etc., and the TTT cure diagram should be a viable option for studying network formation in these bio-based polymers.

Thus, the primary objective of this research is to establish material characteristics, most importantly cure behavior, of polyurethanes derived from lignocellulosics.

The specific objectives to be met are:

1. to examine the differences in the kinetics of isocyanate crosslinking with different lignocellulosic polyols, water, and a synthetic polyol,
2. to examine the gelation and vitrification behavior of lignocellulosic-based polyurethanes,
3. to assess the sensitivity of network formation to variation in resin stoichiometry, and
4. to develop TTT cure diagrams for these bio-based polymers.

CHAPTER 2

2.0 LITERATURE REVIEW

To obtain a comprehensive view of the cure process it is necessary to characterize both the chemistry and physics of crosslinking systems. In conjunction with cure kinetics modelling, such characterization allows for the prediction of cure behavior as a function of formulation variables and time-temperature profiles and for establishing the relationship of cure behavior to end-use properties.

The following review will focus on the topics below, and serve as a basis for interpretation of the experimental results.

- a) Network formation and thermoset cure
- b) Cure characterization techniques
- c) Time-Temperature-Transformation cure diagram

2.1. NETWORK FORMATION AND THERMOSET CURE

2.1.1 Theory of Thermosetting Polymers

Thermosetting polymers or resins are transformed from a mobile liquid to a viscous liquid to an infusible solid during cure. On a molecular level, the cure process can be visualized as converting small molecules to large molecules of high molecular

weight, capable of crosslinking. The latter process is possible only if at least one of the reacting monomer species has a functionality of greater than two.⁴⁸

As thermosetting resins are cured, they pass through three distinct phases. The precursor material (A-stage) is a liquid or solid which is generally soluble and fusible. The precursor passes through a B-stage when it is heated to temperatures which are fairly high. At this stage, chain extension and prepolymer formation take place, yielding a material that is insoluble but that can swell with solvents.^{15,26} The C-stage develops at higher temperatures, and the resulting material is a network which is insoluble and infusible.

The ability of a thermoset to reach the C-stage or form a network is dependent on these critical events: gelation and vitrification. The gel point has been defined as that point in the reaction or cure where the reaction medium undergoes a steep increase in viscosity.⁴⁸ A statistical approach for predicting the extent of reaction at which gelation occurs has been developed.⁵ At any point in the polymerization reaction, a polyfunctional system may be characterized by a branching coefficient, α . This parameter depends on the relative concentration of branch units and bifunctional units and on the extent of reaction (P). A critical branching coefficient, α_c , and a critical conversion, P_c , have been defined as conditions for the occurrence of gelation. The branching coefficient is defined as the probability that a chain segment connected to one branching point is also connected to a second branching point. If this probability is larger than the probability that the chain will terminate as a loose end, the system is a

gel. Vitrification occurs when the material undergoes a transition from a soft rubber to a rigid glass, that is when the rising glass transition temperature (T_g) becomes equal to or surpasses the cure temperature (T_c). The rate of the curing reaction is drastically decreased, and eventually quenched when the resin vitrifies. At this point, the resin had undergone enough crosslinking and attained a high molecular weight to completely immobilize the reactive chains within the network.^{6,7,13,14}

2.1.2 Network-forming Polyurethanes

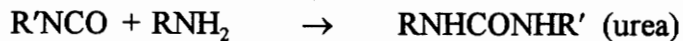
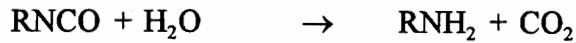
Crosslinked polyurethanes are usually formed by the reaction of a polyfunctional isocyanate with a polyol or other reactant containing two or more groups reactive with the isocyanate group. A comprehensive discussion of the various isocyanate reactions is given by Wright and Cumming,⁴⁹ and by Buist and Gudgeon;⁶ a summary is presented here.

Alcohols or OH-containing compounds react with isocyanates according to the reaction.

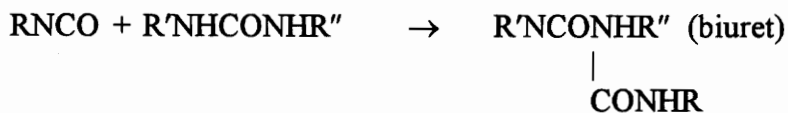


Depending on the nature of the OH-containing compound, a linear or network system is formed. Diols and triols are usually identified with linear and network systems, respectively.

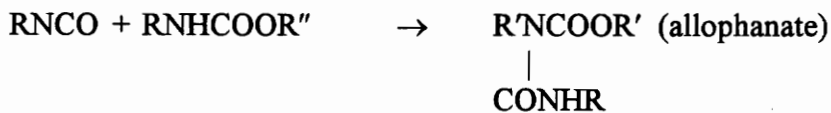
Water reacts with isocyanates, forming amines, the latter reacting with isocyanates to form urea.



This reaction is particularly important in the foam industry. The urea formed, as indicated above, can react with another isocyanate molecule forming biurets. This reaction is significant only at temperatures above 100°C.



At 120°- 140°C, isocyanates react with urethanes, forming allophanates as below:



Biuret and allophanate linkages are reported to affect higher crosslinking in polyurethanes; depending on the molar ratio of NCO to OH in a typical urethane formulation, and temperature, crosslinking could be very significant, due to allophanate and biuret formation.

2.1.3 Parameters Influencing Network Formation

Functionality of Reactants

A network would be formed by a system of molecules having a functionality of greater than two.^{15,47} According to gelation theory, the conversion at gelation decreases with increasing functionality of the reactants.⁴⁷ For a system containing a mixture of $A_1, A_2 \dots A_i$ moles of monomers with functionality $f_1, f_2 \dots f_i$, respectively, and $B_1, B_2 \dots B_j$

moles of monomers with a functionality of g_1, g_2, \dots, g_j , respectively, in which A's can only react with B's, the conversion at gelation, X_{gel} , is given by

$$X_{gel} = \left[\frac{f_c}{g_c} - 1 \right]^{-1/2} \quad (2.1)$$

where $f_c = \frac{\sum_i f_i A_i}{\sum_i f_i A_i}$

$$g_c = \frac{\sum_j g_j B_j}{\sum_j g_j B_j}$$

Chan et al.⁸ have studied the effect of functionality on network formation; gelation and vitrification, using di- and trifunctional epoxy resins, with tetrafunctional aromatic diamine. Figure 1 has been used to explain the experimental results. It is seen that the conversion at gelation decreased with increasing functionality. A parallel situation has been observed for vitrification (graph not shown). Further, the maximum glass transition temperature determined from a series of isothermal cure, showed a positive correlation with increasing functionality.

Molecular weight

Molecules which react at only one site will never contribute to network formation. A molecule connected to a network at two points acts as a chain extender, but not as a junction point, for additional crosslinking. Only molecules which are incorporated into the network with three or more sites contribute as crosslink points.

Kelley et al.²⁴ studied the effect of molecular weight on properties of network polyurethanes (PU). In their study, a series of fractions with number average molecular weight between 1500 to 10,000 daltons, isolated from Kraft hydroxypropylated lignin (HPL), were used as polyols in combinations with hexamethylenediisocyanate (HDI)

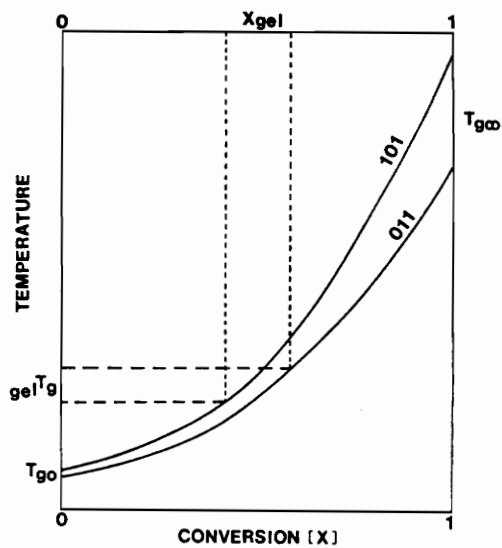


Figure 1. A schematic diagram of T_g vs conversion at vitrification for reactants differing in functionality ($101 > 011$). The conversions at gelation are also included. The diagram is useful for demonstrating the effect of increasing functionality on gelation, vitrification and the temperature, $T_{g,0}$, $T_{g,\infty}$, and gel T_g .

to prepare solvent-cast PU films. The DMTA spectra of their PU network is shown (Figure 2). The T_g of the polymer has been determined as the maximum peak of the $\tan \delta$ curve, which coincided with a sudden drop in the modulus. As the molecular weight of the lignin fraction is increased, the T_g increased in a consistent fashion.

Further characterization of their film was made using swelling experiments. Swelling data permitted the determination of molecular weight between crosslinks (M_c) according to the Flory-Huggin equation 2.2:

$$M_c = \frac{V_s P_p [C^{0.33} - \frac{c}{2}]}{\ln[1 - c] + c + Xc^2} \quad (2.2)$$

where

V_s = molar volume of solvents used for swelling the polymer

P_p = density of polymer

X = Flory-Huggin constant

c = relative concentration = $\frac{W_D}{P_p V_\infty}$

W_D = dry weight of polymer

V_∞ = final swollen volume of polymer, which is given by

$$V_\infty = \frac{W_D}{P_p} + \frac{W_\infty - W_D}{P_s}$$

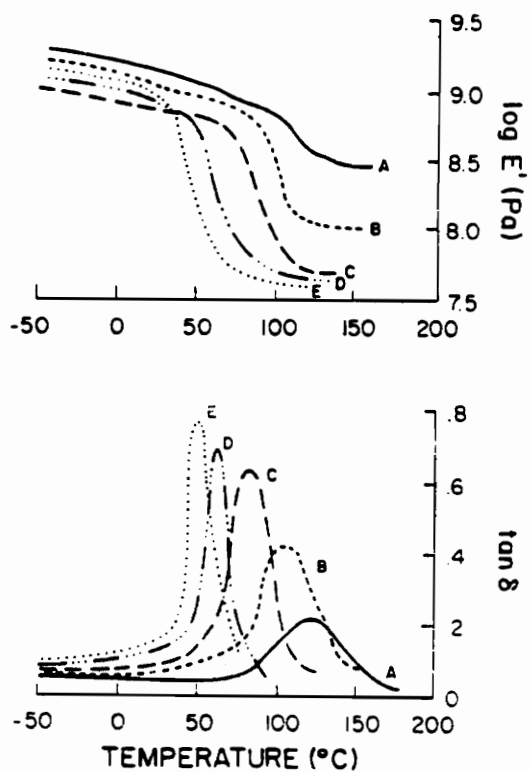


Figure 2.

A DMTA spectrum depicting the effect of increasing molecular weight on the T_g of polyurethanes from lignin fractions. The order of increasing molecular weight is as follows $A > B > C > D > E$. The peak of the $\tan \delta$ is taken as the T_g .

W_{∞} = weight of swollen polymer

P_s = density of solvent

Percent sol fraction and swell were calculated as follows

$$\text{Sol fraction} = \frac{W_{\infty} - W_D}{W_o} \times 100\% \quad (2.3)$$

$$\text{Percent swell} = \frac{W_{\infty} - W_D}{W_D} \quad (2.4)$$

W_o is the initial weight of polymer.

In their work, and in general, it is necessary to determine the Flory-Huggin's constant, X , for the polymer-solvent systems. This was determined by running a series of swelling tests at different temperatures. From the temperature dependency of the swelling volume, V_{∞} , X was obtained as follows

$$\frac{d \ln V_{\infty}}{d \ln T} = \frac{-3X[1 - V_{\infty}]}{5(1 - X)} \quad (2.5)$$

where T = absolute temperature.

Molecular weight between crosslinks, percent swell, and sol fraction have been reported to vary inversely with the molecular weight of lignin.

Resin Stoichiometry

The relative proportions or molar ratio of reactants has been reported to affect network formation by several scientists. The molar ratio of phenol to formaldehyde,

coupled with the reaction medium, is reported to affect crosslinking in phenol formaldehyde resins. In an alkaline medium, and a molar excess of formaldehyde over phenol, PF resins form a network during cure; when the opposite situation exists, no network is formed.¹ In the former, there are unreacted methanol groups which can condense to form a crosslinked structure. However, in the other case, there are no unreacted methanol groups and thus crosslinking is not possible.

Kelley et al.²⁴ and Yoshida et al.⁴⁶ have reported on the effect of isocyanate to hydroxyl ratio on the properties of lignin-based polyurethanes. Molecular weight between crosslinks of these polymers was calculated from swelling data, as done by Kelley et al., and converted into crosslink density as follows:

$$C = P_p/M_c \quad (2.6)$$

C = crosslink density in moles per cubic centimeters

P_p = density of polymer

M_c = molecular weight between crosslinks

The use of excess of isocyanate over stoichiometry influences network formation in polyurethanes. Low NCO to OH ratio favors the formation of urethane linkages only, while high NCO to OH ratio at the appropriate temperature favors the formation of urethane, and allophanate linkages, the latter being responsible for additional crosslinking.

Temperature

Gillham et al.¹⁷ and Hoffman^{19,20} have reported on the effect of cure temperature on crosslinking. The degree of conversion at gelation is constant, regardless of cure temperature; however, conversion at vitrification varies linearly with increasing cure temperature. Typical DMTA spectra (from reference 19) are shown (Figure 3). The two $\tan \delta$ maxima have been labelled as gelation and vitrification. At lower temperatures, in the range of 30-50°C, the single $\tan \delta$ peak indicates that vitrification takes place before the necessary conversion into a gel has been reached. A splitting of the peak can be observed at approximately 60°C. The gap between the peaks widens with increasing cure temperature. The higher the cure temperature, the earlier both gelation and vitrification. Gillham et al. have used the TBA and similar observations have been made, details can be found elsewhere.¹⁶⁻¹⁸

2.2 CURE CHARACTERIZATION TECHNIQUES

The cure process has been described as the conversion of small molecules to large ones through the process of chain extension, branching and crosslinking, usually with the buildup of a three-dimensional network of infinite molecular weight. To obtain a detailed understanding of the cure process, it is necessary to characterize both the physics and chemistry of the crosslinking systems.^{34,36} Some of the cure characterization methods are listed, with a review of the most commonly used ones.

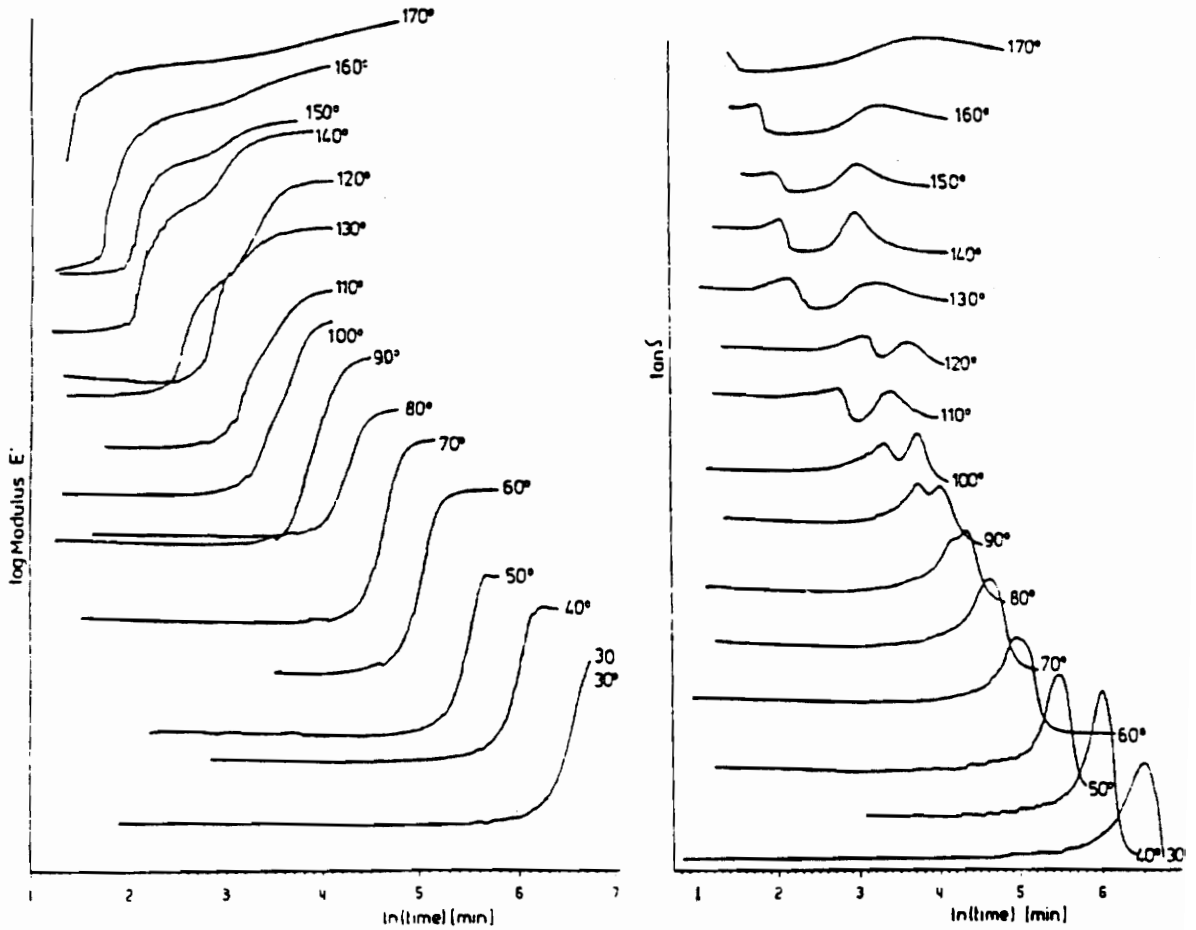


Figure 3. DMTA spectra of an epoxy resin depicting the variation of vitrification and gelation with cure temperature

The problem with cure studies of thermosets is that the material may pass through several distinct stages: liquid to rubbery to glassy state. Frequently, a technique is sensitive to only one of these curing regimes, and a comprehensive characterization may involve the use of several techniques.

2.2.1 Chemical Methods

- Differential scanning calorimetry (DSC)

- Fourier transform infrared (FTIR) spectroscopy

- Solid-state nuclear magnetic resonance (NMR) spectroscopy

- Viscosity measurement

- Swelling experiment

2.2.2 Physical Methods

- Dynamic mechanical thermal analysis (DMTA)

- Thermogravimetric analysis (TGA)

- Dielectric thermal analysis (DETA)

2.2.1 Viscosity Measurement

Viscosity measurement is often used as a criterion for determining the endpoint of a resin synthesis procedure. It may therefore provide useful information about the degree of advancement of the resin before it is further cured. It is a measurement which is insensitive to the latter stages of cure. It can no longer be practically determined when a thermoset has gelled and has developed a highly crosslinked network, at which point the viscosity of the curing system is infinite.⁴⁷ Nevertheless,

it has been used in cure studies of some systems. Reboledo et al.³⁷ have studied thermosetting polyurethanes using viscosity measurements to the gel point. In their work, the viscosity of the polymerizing mixture was best characterized by the weight-average molecular weight (M_w), since both parameters become infinite at the gel point. In order to find a correlation of viscosity with the weight average molecular weight, the latter quantity was related to the fractional conversion, determined by finding the percent NCO content with time, using the network polymerization theory proposed by Macosko and Miller,²⁷ expressed mathematically as

$$\frac{M_w}{M_{w_0}} = 1 + \frac{x f_p [x [f_p - 1] M_I^2 + x [f_I - 1] M_p^2 + 2 M_I M_p]}{M_{w_0} M_p [1 + M_I / M_p] [1 - x^2 (f_p - 1) (f_I - 1)]} \quad (2.8)$$

where M_{w_0} = initial weight-average molecular weight

M_I and M_p are the molecular weights of the isocyanate and polyol, respectively.

M_I / M_p is the initial mass ratio. f_p and f_I are the functionality of

polyol and isocyanate, respectively. X = conversion at gel point.

The viscosity was then related to weight average molecular weight as

$$\frac{n}{n_0} = \left(\frac{M_w}{M_{w_0}} \right)^m \quad \text{where } m \text{ is an integer found as the slope of a plot of } n/n_0 \text{ versus}$$

$\frac{M_w}{M_{w_0}}$ on a logarithmic scale.

Swelling Experiments

This technique is based on the degree of swelling of polymers as they increase in size during the progression of the curing reaction. It involves swelling a cured polymer film of known weight in a suitable solvent, usually DMF, for a specified period, and recording the final swollen weight. The swelling data can be converted to parameters such as molecular weight between crosslinks, crosslink density, sol fraction and percent swell. The various mathematical procedures have been discussed under the effect of molecular weight on network formation and will not be reproduced here.

FTIR

This technique has been frequently used to follow the cure of thermosets. It is based on the fact that each chemical group present in a sample absorbs infrared radiation of a characteristic frequency. The amount of radiation absorbed relative to the amount of radiation incident on the sample can be related directly to the concentration of the absorbing species by²²

$$A = \alpha Lc \quad (2.8)$$

where A is the absorbance, α = absorptivity, which is characteristic of the absorbing species, L = sample thickness and C is concentration of the absorbing group. The key

to the use of FTIR to monitor cure is the assignment of absorption bands to functional groups that appear or disappear during the progression of the curing reaction. During the reaction, however, the thickness of the sample may change due to temperature variations or density changes caused by the reaction itself. To compensate for these changes, a ratio is taken between the absorbance of a group of interest and that of an internal standard, a group whose concentration does not change during the reaction.²²

Several scientists have used the absorption band at 2200-2300 cm⁻¹ characteristics of the isocyanate N=C stretch to follow the cure of polyurethanes^{12,21,36} based on the assumption that the change in the NCO concentration with reaction time is due only to the reaction between the NCO and an OH group. The C-H absorption band at 2650-3030 cm⁻¹ has been used as the internal standard in all cases. Owusu et al.³² have studied cyanate ester resin systems, and have used the decrease of the cyanate vibration at 2270 cm⁻¹ to monitor cure, and the C-H stretch at 2950 cm⁻¹ as an internal standard.

The fraction of unreacted functional group has been calculated as follows

$$C(t) = \frac{A[t]_x A(o)_j}{A(o)_x A(t)_j} \quad (2.9)$$

where $A[t]_x$ is the absorbance of the group of interest at time t, $A(t)_j$ is the absorbance of the internal standard at time t and $A(o)$ the initial absorbance. $C(t)$ is fraction of

unreacted functional group. The data has been analyzed using an empirical equation of the form

$$\frac{dc}{dt} = -kC^n \quad (2.10)$$

where k is the rate constant and n is the order of reaction.

In both cases, a second order reaction has been reported. Although FTIR involves a direct measure of curing chemistry, there are some limitations to it. The events that take place in the latter stages of cure are difficult to detect by FTIR. There are also conflicts in the literature over the assignment of absorption bands to the various functionalities.

Differential Scanning Calorimetry (DSC)

DSC is an important thermal technique which has been used extensively to follow the curing chemistry of thermoset resins. DSC measures the exothermic or endothermic behavior of a small sample as it is subjected to a continuously increasing temperature.^{9,29,34} In the DSC experiment, a thermocouple placed underneath an encapsulated sample is used to detect a temperature difference between the sample and an inert reference material. Heat is supplied to either the sample or reference material to maintain the two at identical temperatures.

Kinetic Analysis by DSC

The underlying assumption of kinetic studies by DSC is that the rate of exothermic heat, as recorded as a function of time or temperature, is proportional to the

rate of conversion and that thermal gradient within the sample or reference material is negligible. The former is true as long as no other thermal events, e.g. melting or crystallization, occur at the same time, and the latter could be achieved with sample sizes in the order of 5-10 mg.

Rates of conversion and partial conversion, i.e. rate of cure, could be extracted from DSC using these equations.¹¹

$$\frac{d\alpha}{dt} = \frac{\left[\frac{d\Delta H}{dt} \right]}{\Delta H_{r\infty n}} \quad (2.11)$$

$$\alpha_t = \frac{(\Delta H)_t}{(\Delta H)_{r\infty n}} \quad (2.12)$$

where $d\alpha/dt$ is the rate of conversion

α_t is partial conversion

ΔH_t is heat evolved at time t

$\Delta H_{r\infty n}$ is total heat evolved

DSC can be carried out in isothermal and scanning mode, and kinetic data can be obtained from both techniques. The former is more straight-forward; rate and extent of cure are recorded only as a function of time, while in the latter case these parameters are simultaneously determined as a function of time and temperature. Isothermal experiments also provide the maximum cure attainable at a particular cure temperature. The disadvantage of isothermal mode is that the recorded traces show an initial data uncertainty due to the necessary heating of the sample to the desired cure temperature.

This is particularly true of n^{th} order reactions, which exhibit their maximum rate of conversion at the very beginning of the reaction. For instance, Mussati²⁹ attempted a DSC study of network-forming polyurethanes, and found out that by the time the sample attained the cure temperature, a significant portion of the reaction had occurred. Since freezing the system to arrest the reaction prior to testing in the DSC produced phase separation, an accurate integration over the rate of heat release versus time curve was not possible. Consequently, a confirmation of the kinetics could not be made using the DSC.

DSC in scanning mode with multiple heating is a suitable alternative. The use of this form to study kinetics of cure has been pioneered by Ozawa et al.^{11,35} Ozawa's method combines two equations; the basic rate equation that relates the rate of conversion $d\alpha/dt$ at constant temperature to the concentration of reactants $f(x)$ through a rate constant k as

$$\frac{d\alpha}{dt} = k[f(x)] \quad (2.13)$$

and the Arrhenius relationship

$$K = A \exp [- E/RT] \quad (2.14)$$

where E is activation energy, R is gas constant, T is absolute temperature and A is frequency factor.

The combined equation is

$$\frac{d\alpha}{dt} = f(x)A\exp\left[-\frac{E}{RT}\right] \quad (2.15)$$

Integration of this equation yields

$$\int_0^{x_p} \frac{dx}{f(x)} = A \int_{t_0}^{t_p} e^{-E/RT} dt \quad (2.16)$$

when T/θ is substituted for t , where θ is the heating rate, the equation takes the form

$$\frac{A}{\theta} \int_{T_0}^{T_p} e^{-E/RT} dT \approx \frac{A}{\theta} \int_0^{T_p} e^{-E/RT} dT \approx \frac{AE}{\theta R} P[E/RT] \quad (2.17)$$

Values for $P(E/RT)$ have been tabulated by Doyle¹¹ where $\text{Log}_p[E/RT] \approx -2.315 - 0.4567 E/RT$ for $20 < E/RT < 60$.

Under the assumption that X_p , conversion at the peak temperature (T_p) is constant, and independent of heating rate, that is

$$\int_0^{x_p} \frac{dx}{f(x)} \text{ is constant}$$

a plot of log heating rates versus the reciprocal of peak temperature (for each heating rate), i.e. $\log\theta$ vs T_p^{-1} , allows for determination of the activation energy of a system under study. This plot is referred to as Ozawa's plot.

The frequency factor (A) for n^{th} order reactions is given by

$$A = \frac{\emptyset E \exp [E/R T_p]}{R T^2 p} \quad (2.18)$$

Thus using \emptyset , T_p and the resulting E from Ozawa's plot, it is possible to determine A and the rate constant k . The combined equation [Ozawa's equation] can be recast in an Arrhenius form as

$$\ln[Af(x)] = \ln \left[\frac{d\alpha}{dt} \right]_T + \frac{E}{RT} \quad (2.19)$$

where $\left[\frac{d\alpha}{dt} \right]_T$ is the rate of conversion at temperature T . Assuming a second order reaction (i.e. $f(x) = (1 - x)^n$), a plot of $\ln[Af(x)]$ versus $\ln[1 - x_T]$ would permit determination of the order of reaction [the slope].

Hofmann¹⁹ has studied the cure kinetics of lignin-based epoxy resins using Ozawa's method. His results are in good agreement with those reported from TBA studies.

2.2.2 Dynamic Mechanical Thermal Analysis (DMTA)

DMTA measures the tendency of a polymeric material to store or dissipate mechanical energy when it is subjected to a small oscillatory stress.^{34,35,43} If a material is perfectly elastic, the resulting deformation or strain is exactly in phase with the applied stress. When the applied frequency matches the reciprocal of the relaxation time of a characteristic molecular motion, the strain response lags behind the stress.³⁰ The time lag measured between stress and strain can be characterized by a phase angle,

δ . When δ becomes very large, the material is said to exhibit a high degree of damping behavior. In high damping materials, much of the energy used to deform the material is dissipated directly into heat. If the material exhibits little or no damping, it snaps back immediately when the applied stress is taken away.

DMTA results are expressed in terms of complex moduli, E^* , which is resolvable into elastic and viscous components called storage moduli (E') and loss moduli (E''), respectively. A single parameter that expresses the relative importance of viscous to elastic behavior is $\tan \delta$. Physically, $\tan \delta$ is the tangent of the phase angle lagging between the stress and strain. The following equations express the mathematical relationship between these four parameters

$$E^* = E' + E''$$

$$\tan \delta = E''/E'$$

The most comprehensive study of thermoset cure using the DMTA is that published by Hofmann^{19,20}, Niranjan³¹, and Follensbee et al.¹⁴. Data analysis of DMTA results is similar to those of TBA and is discussed in Section C.

Cure Kinetics by DMTA

During a temperature scan, the modulus will increase in the curing temperature region for a thermoset system (Figure 4). Provder et al.³⁵ have related this increase in modulus to the fractional extent of cure, $F(t,T)$, and defined it as follows

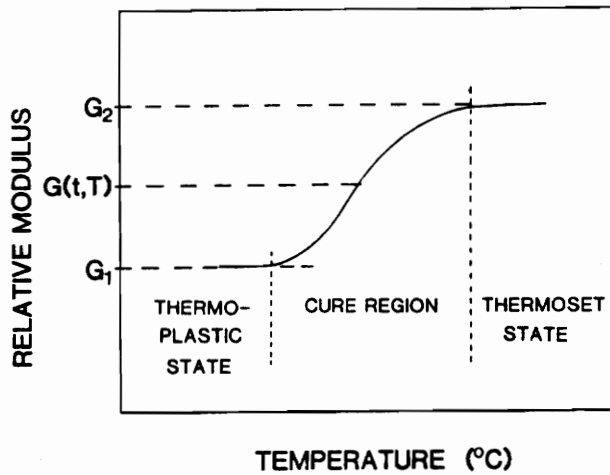


Figure 4. A hypothetical DMTA relative modulus profile as a function of temperature during cure. Fractional cure is obtained at any point in the cure region according to equation 2.20.

$$F(t,T) = \frac{G(t,T) - G_1}{G_2 - G_1} \quad (2.20)$$

where G_1 , $G(t,T)$ and G_2 are modulus readings at the onset of cure, at a given time and temperature during the cure process, and after the cure process has ceased, respectively.

Equation (1) has been subjected to a general n^{th} order rate expression as follows

$$\frac{dF}{dt}(t,T) = k(T)[1 - F(t,T)]^n \quad (2.22a)$$

where n is the order of reaction, the rate constant $k(T)$ takes on the form

$$k(T) = \frac{1}{\phi} \frac{dF(t,T)}{dT} [1 - F(t,T)]^{-n} \quad (2.22b)$$

where ϕ is the heating rate, dT/dt , $[dF(t,T)]/dT$ is the rate of change of degree of cure with respect to temperature.

Generally, the rate constant is related to temperature in an Arrhenius expression as

$$\ln k(T) = \ln A - \frac{E}{RT} \quad (2.23)$$

A is the Arrhenius frequency factor, E is the activation energy, R is the gas constant.

Equations (2.22) and (2.23) can be related by the equation below

$$\ln A - \frac{E}{RT} = \ln \frac{1}{\phi} \frac{dF(t,T)}{dT} [1 - F(t,T)]^{-n} \quad (2.24)$$

From equation (2.24), it is possible to compute a series of rate constant values following a cure profile (Figure 4).

The order of reaction (n), the only unknown value in equation (2.24), is selected by evaluating the linearity of the Arrhenius plot $\ln k(T)$ versus $1/T$.

In the case of an isothermal cure, where the x-axis (Figure 5) is in time domain, fractional degree of cure could be derived in a similar fashion; equation (2.20), the integral form of equation (2.22) is used to examine the kinetics of the cure reaction as follows:

$$[1 - n][(1 - F)^{1-n} - 1] = k(T)t \quad n \neq 1 \quad (2.25a)$$

$$-\ln(1 - F) = k(T)t \quad n = 1 \quad (2.25b)$$

By plotting the lefthand side of equation (2.25a) or (2.25b), as a function of time, a straight line indicates the reaction order, and the slope gives the reaction rate constant $k(T)$.

Time-Temperature Prediction of Cure

As noted in equation (2.22), for curing reactions following n-th order kinetics, the rate of cure, dF/dt is related to the uncured fraction (1-F) as follows

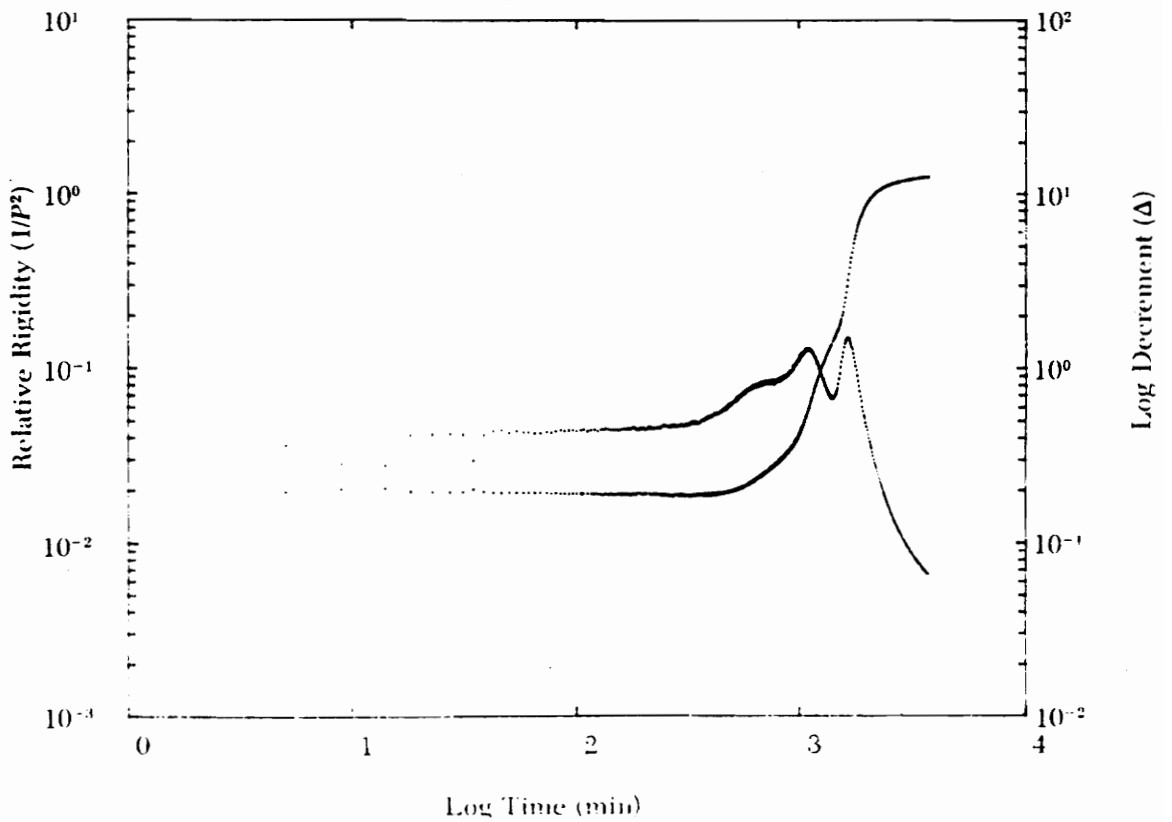


Figure 5. An isothermal cure profile of an epoxy resin. The two prominent peaks are identified as gelation and vitrification.

$$\frac{dF}{dt} = A \exp\left[-\frac{E}{RT}\right][1-F]^n, \text{ where the rate constant}$$

$$k = A \exp\left[-\frac{E}{RT}\right], \text{ integration of this equation gives}$$

$$F(t,T) = 1 - [(n-1)k(T)t + 1]^{\frac{1}{1-n}} \quad n \neq 1 \quad (2.26)$$

The above equation relates the degree of cure, F, to the cure (t) and temperature (T). It is therefore possible to predict the degree of cure at any desired set of t-T values, provided the activation energy and the pre-Arrhenius factor are known.

Torsional Braid Analysis

This technique has been used extensively for thermoset cure studies, and is the most reported technique for the construction of the TTT cure diagrams¹⁵⁻¹⁸, and would be discussed in Section C.

2.3 TIME-TEMPERATURE-TRANSFORMATION CURE DIAGRAMS

The transformation of low molecular weight liquid into high molecular weight amorphous solid polymer by isothermal chemical reaction is the fundamental process used in the coatings, adhesives and thermoset industries. As the chemical reaction proceeds, the molecular weight and T_g increases, and if the reaction is carried out below the glass transition temperature of the fully reacted system ($T_{g\infty}$), the polymer T_g will eventually equal the reaction or cure temperature (T_c).¹⁶ During isothermal reaction

below T_{gco} , two phenomenon of critical importance in thermoset are gelation and vitrification^{8,9,15-18}. If a series of isothermal cure experiments is performed, and the cure temperature is plotted against the times to gelation and vitrification, then an isothermal time-temperature-transformation (TTT) cure diagram is obtained.¹⁶

The TTT cure diagram provides a framework for understanding the cure process of thermosetting materials. Relationship between cure, structure, and properties can also be understood by studying the TTT diagram. Such a diagram for thermosets would permit time-temperature paths of cure to be chosen so that gelation and vitrification occur in a controlled manner and consequently give rise to predictable properties of the thermosetting matrix.¹⁶⁻¹⁸

2.3.1 A Schematic TTT Cure Diagram

A schematic TTT cure diagram is shown (Figure 6). The diagram indicates distinct regions of matter encountered in the cure of thermosets; these include liquid, sol/gel rubber, elastomer, gelled glass, ungelled glass and char. Three critical temperatures are also shown: T_{go} , T_{gg} , and T_{gco} . A full cure line is indicated on the diagram in the gelled glass region; this line also separates the sol/gel rubber and elastomer regions above T_{gco} . T_{go} is the glass transition temperature of the uncured resin. Below this temperature, in principle the system has no reactivity.

T_{gg} is the temperature at which gelation and vitrification coincide. Below T_{go} and T_{gg} , the system will vitrify before gelling, in principle quenching the chemical reactions, and thus precluding gelation. At vitrification below T_{gg} , the system is of

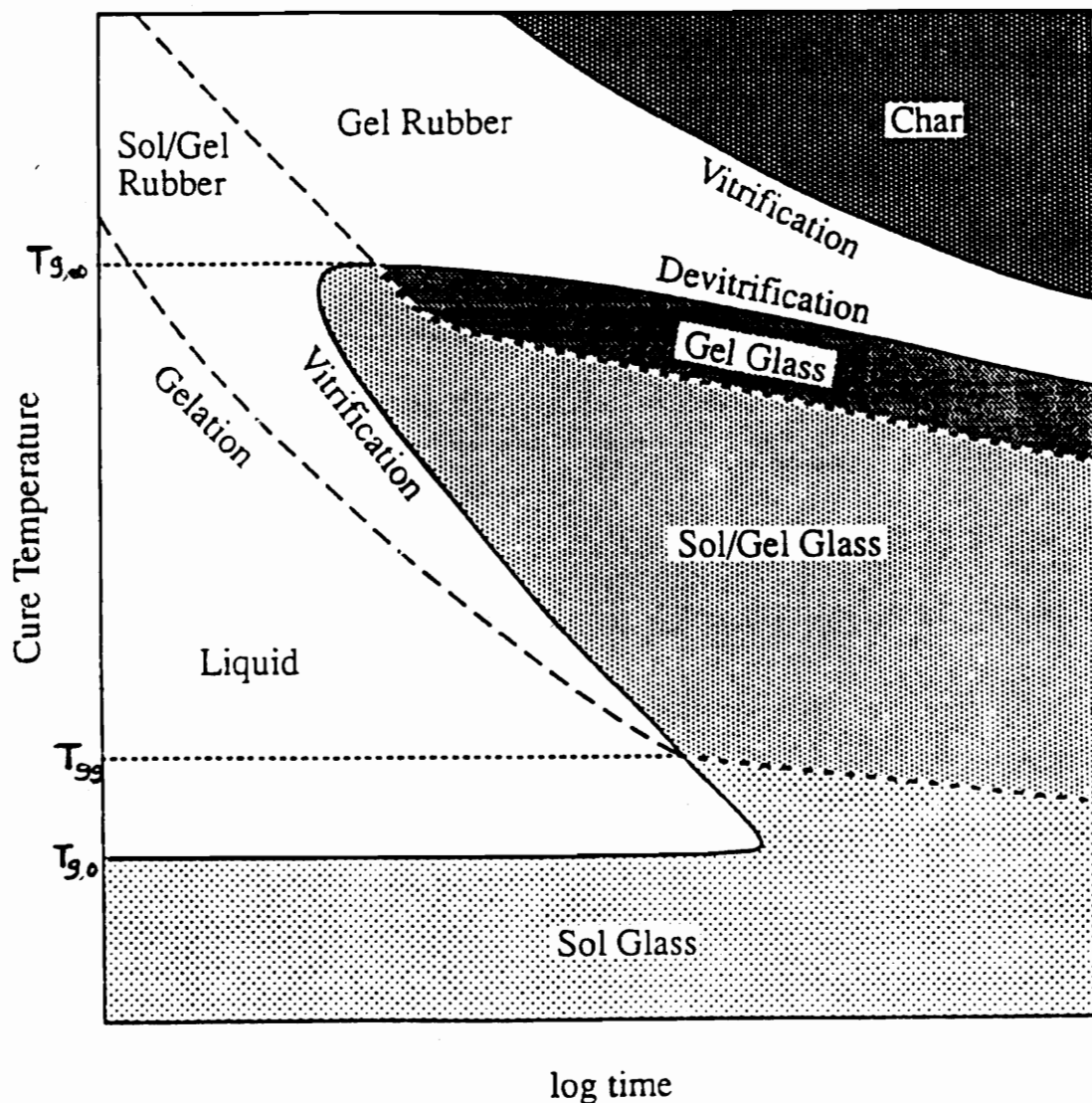


Figure 6. A schematic TTT cure diagram for a thermosetting polymer showing the different states encountered during cure. $T_{g,o}$, T_{gg} and $T_{g,\infty}$ are the glass transition temperature of the reactants, the temperature at which times to gelation and vitrification are the same, and the glass transition temperature of the fully reacted system, respectively.

low molecular weight, and on subsequent heating the material will flow and is processable.^{8,9,16}

$T_{g\infty}$ is the maximum glass temperature of the system. Between T_{gg} and $T_{g\infty}$, the material is initially in the liquid region, and is soluble and of low molecular weight. On further reaction, gelation occurs, and the sol/gel rubber region is entered. Finite molecular sol and infinite molecular weight gel form a miscible binary mixture in this region.¹⁶

Eventually, T_g will rise to T_c , and vitrification is said to occur. Vitrification greatly decreases the mobility of the molecules, and thus in principle the chemical reactions are quenched. Recent work has investigated the cure behavior after vitrification and has shown that reactions do occur in the glassy state on prolonged isothermal cure beyond vitrification.⁸ The full cure line in the figure is the time required at any given T_c , for the T_g to equal $T_{g\infty}$ in a subsequent dynamic scan after the isothermal cure. The determination of the full cure line is important because meaningful structure-property relationships between different systems can only be made by considering fully-cured materials. For systems where $T_{g\infty}$ can be attained in the absence of degradation, curing above $T_{g\infty}$ is the most direct method of achieving full cure. For systems where curing above $T_{g\infty}$ would lead to degradation, the full cure line presents an alternative for achieving complete cure.^{3,8,16,17}

A rubber is formed above $T_{g\infty}$ after prolonged isothermal cure. At high temperatures, thermal degradation becomes important and may prevent full cure from being achieved.⁸

Two degradation events have been identified: devitrification followed by rubber formation, and vitrification followed by char formation.⁸ The devitrification event corresponds to a decrease in T_g from above to below isothermal T_c . The second event is a rubber to glass transformation, accompanied by an increase in T_g and rigidity and is presumably the onset of char formation.⁸

2.3.2 Experimental Aspect of the TTT Cure Diagram and Data Interpretation

The isothermal TTT cure diagram summarizes the transitions that occur during isothermal polymerization, such as vitrification, gelation and devitrification. Typically, the cure process must be followed from the initial liquid state, through gelation and the sol/gel rubber region, and into the solid vitrified region. The cured material is then subjected to a temperature scan at a fixed scanning rate in order to determine the T_g and other transition temperature after cure. A technique that has been used extensively to study and construct TTT cure diagrams is the TBA.^{8,9,16-18} In this technique, a resin-impregnated fiberglass braid is subjected to damped torsional oscillations, whereby the logarithmic increment of successive amplitudes, $\Delta = \log [A_j/A_i + 1]$, is a measure of energy dissipation or damping of the material, and the relative rigidity [$1/p^2$, p is the period] is a measure of sample stiffness.^{8,9,16-18}

Hofmann^{19,20} and Niranjani³¹ have shown that it is possible to use the DMTA to study and construct the TTT cure diagram and are the only case found in the literature. In this case, the resin-impregnated fiber braid is subjected to forced oscillations of constant frequency in bending, shear or torsion. Loss (E'') and storage (E') moduli are recorded and the $\tan \delta$ characteristics of material damping is obtained as E''/E' . The relative rigidity in the TBA is proportional to E' and log decrement is proportional to $\tan \delta$. The TBA or DMTA is interfaced with a temperature controller that permits isothermal, linearly increasing and decreasing temperature modes. A typical TBA spectrum is shown (Figure 5). The two most important prominent peaks are labelled as gelation and vitrification.

In order to construct a TTT cure diagram, a series of isothermal cures is performed at different temperatures, and the relative rigidity or E' and log decrement or $\tan \delta$ recorded as a function of time.¹⁶ After extended isothermal cure, the system is cooled from the T_c to a selected subambient temperature, say $-T^\circ\text{C}$, heated from that temperature to a specified post-cure temperature, and then immediately cooled to $-T^\circ\text{C}$. The initial scans from $-T^\circ\text{C}$ to the post-cure temperature yields the T_g after cure, which is usually observed to be greater than T_c . The subsequent scan from the post-cure temperature to $-T^\circ\text{C}$ yields the $T_{g\infty}$ for that particular cure temperature (T_c). $T_{g\infty}$ of the system is obtained by averaging the values of $T_{g\infty}$ for different cure temperatures.

A temperature scan of the uncured resin, usually from subambient gives the value of T_{g0} . Determination of T_{gg} involves plot of times to vitrification and gelation

versus cure temperature, and extrapolation of the curves to a point where they coincide. This is illustrated (Figure 7). This procedure has been employed by Hofmann^{19,20} and Gillham and Benci.¹⁸

The times to gelation (t_{gel}) and vitrification (t_{vit}) have been determined by many using these equations^{8,9,16-20}

$$t_{gel} = Ae^{E/RT} \int_0^{\alpha_{gel}} \frac{dx}{f(x)} = Ae^{E/RT} \left[\frac{1}{1-\alpha_{gel}} - \ln \left[\frac{1-\alpha_{gel}}{\alpha_{gel}} \right] \right] \quad (2.27)$$

$$t_{vit} = Ae^{E/RT} \int_0^{\alpha_{Tg}} \frac{dx}{f(x)} = Ae^{E/RT} \left[\frac{1}{1-\alpha_{Tg}} - \ln \left(\frac{1-\alpha_{Tg}}{\alpha_{Tg}} \right) \right] \quad (2.28)$$

- where A = frequency factor
 E = activation energy
 α_{gel} = conversion at gelation
 α_{Tg} = conversion at T_g

α_{Tg} can be calculated using the DiBenetetto⁷ equation that is

$$\alpha_{Tg} = \frac{T_g - T_{g_0}}{T_{g_0}(E-F) + (T_g - T_{g_0})(1-F)} \quad (2.29)$$

The parameters E and F are material constants of the polymer and are determined empirically. α_{gel} can be calculated by gelation theory, discussed earlier. A second method, which is easier for the determination of times to gelation and vitrification has been used by Gillham and Benci¹⁸ and is illustrated (Figure 8). The

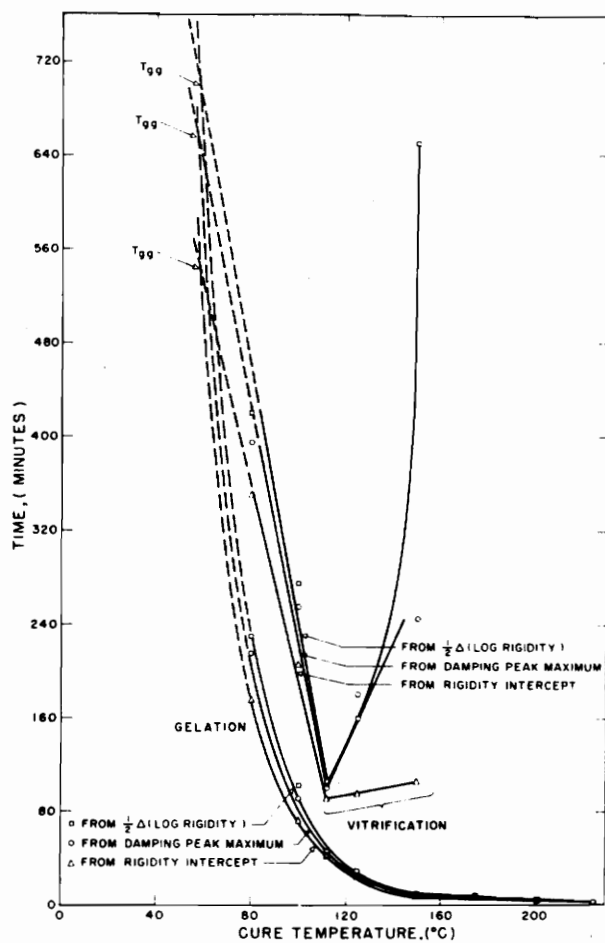


Figure 7. Time to gelation and time to vitrification vs temperature of isothermal cure. Gelation and vitrification times were obtained by the three methods shown in Figure 8. This diagram is useful for determining the temperature at which gelation and vitrification coincide, at T_{gg} .

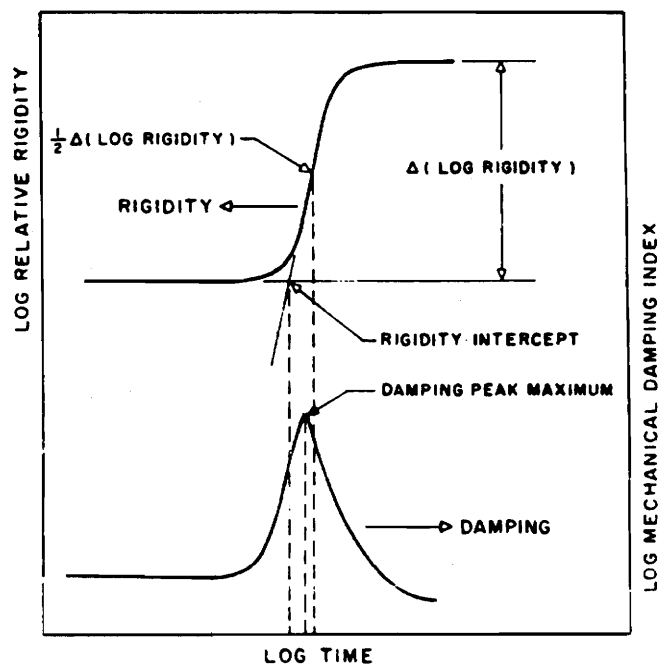


Figure 8. Methods for determining times to gelation and vitrification. Top: rigidity and $\frac{1}{2}\Delta$ (log rigidity) from the relative rigidity curve. Bottom: clamping peak maximum from the damping curve. The time at which the damping peak maximum, $\frac{1}{2}\Delta$ (log rigidity), is the time to gelation or vitrification, depending on cure temperature.

damping peak maximum, $\frac{1}{2}\Delta(\text{Log rigidity})$, and rigidity intercepts are used to define times to gelation or vitrification.

2.3.3 Time-temperature shift of T_g versus time

For slow to moderately reactive systems, it would be quite impractical to construct complete vitrification curve in the TTT cure diagram, especially at low temperatures since the material would take a considerable time to vitrify. And for some thermoset systems (e.g., lignin-based epoxy), damping typical of vitrification is absent, making it impossible to define time to vitrification. Wisanrakkit and Gillham³⁶ have utilized the T_g as a parameter to monitor isothermal cure of thermoset systems and the mathematical model is presented.

For a kinetically controlled reaction, the reaction rate is described by the kinetic rate equation:

$$\frac{dx}{dt} = k(T)f(x) \quad (2.30)$$

where $k(T)$ is the reaction rate constant which is a function of temperature only. $f(x)$ is some function of conversion and t is cure time.

Rearranging equation (2.30), integrating at constant temperature, and taking the natural logarithm

$$\ln \left[\int_0^x \frac{dx}{f(x)} \right] = \ln k(T) + \ln t \quad (2.31)$$

The lefthand side of this equation is a function of conversion only and equivalently, therefore, a function of T_g only, i.e., $F(tg)$.

Therefore

$$F(T_g) = \ln k(T) + \ln(t) \quad (2.32)$$

This equation describes the variation of T_g with cure time and temperature. Let T_g vary with time, t_1 , for cure temperature T_1 and with time t_2 for cure temperature T_2 .

$$F(T_g) = \ln k(T_1) + \ln(t_1) = \ln k(T_2) + \ln(t_2) \quad (2.33)$$

$$\ln(t_1) - \ln(t_2) = \ln k(T_2) - \ln k(T_1) \quad (2.34)$$

For any two isothermal temperatures, $\ln k(T_2) - \ln k(T_1)$ is a constant. Therefore, for a kinetically controlled reaction, the variation of T_g with time at two different cure temperatures (T_1 and T_2) when plotted as a function of $\ln(\text{time})$ will have the same functional form except that the curve for the cure temperature T_2 will be displaced from that of the temperature T_1 by a constant factor. It follows that, if the reaction is solely kinetically controlled, T_g versus $\ln(\text{time})$ curves at different cure temperature should be superimposed by simply shifting each curve along the $\ln(\text{time})$ axis relative to a curve at an arbitrary reference temperature by a shift factor, $A(T) = \ln(t_{ref}) - \ln(t_T)$, for each temperature relative to the reference temperature.

The shift factors, $A(T)$, can be used to calculate the Arrhenius activation energy for the reaction since equation 2.35 provides the relationship between the time shift factors and the rate constants:

$$A(T) = \ln(t_{ref}) - \ln(t_T) = \ln k(T) - \ln k(T_{ref}) \quad (2.35)$$

$$= -\frac{E}{RT} + \frac{E}{RT_{ref}} \quad (2.36)$$

A plot of the shift factor against $1/T$ should yield a straight line with slope given by $-E/R$ and intercept $E/R(T_{ref})$. The relationship between the times to reach a fixed T_g at different cure temperatures for a kinetically controlled reaction is given by equation 4, recast as follows

$$-\frac{E}{RT_1} + \ln(t_{T_{g_1}}) = -\frac{E}{RT_2} + \ln(t_{T_{g_2}}) \quad (2.37)$$

where $t_{T_{g_1}}$ is the time needed to reach a given glass transition temperature, T_{g^*} , at cure temperature T_1 and $t_{T_{g_2}}$ is the time needed to reach the same T_g at cure temperature T_2 . Thus, if a time to reach a particular T_g at one cure temperature is known, then the times to reach the same T_g at different temperature can be calculated from equation (2.37) provided the activation energy is known.

The times to reach a fixed T_g at different cure temperatures when plotted as T_{cure} versus cure time constitute an iso- T_g line in the TTT cure diagram.

When T_2 is equal in value to the glass transition temperature T_{g^*} , the time $t_{T_{g_2}}$, calculated from equation (2.37) is the time to reach isothermal vitrification.

Vitrification points for all possible values of T_g , when plotted in the form of T_c versus cure time, constitute the vitrification curve in the TTT diagram.

CHAPTER 3

3.0 MATERIALS AND METHODS

3.1 MATERIALS

3.1.1 Isocyanates

The isocyanate used was polymeric methylene diphenyl diisocyanate, obtained from ICI polyurethanes, and used as received. This isocyanate is sold under the trade name Rubinate MF-184.

3.1.2 Polyols

The OH-containing compounds used in the study are as follows:

- a) Caprolactone triol (CPL). This was obtained from Aldrich Chemicals and was dried over molecular sieves prior to use.
- b) Hydroxypropyl cellulose (HPC). This was obtained from Hercules and is sold under the trade name Klucell.
- c) Hydroxypropyl lignin (HPL). This was obtained from the pilot plant at the Forest Products department, Virginia Tech.

HPC and HPL were dried under a 30mm/Hg vacuum at room temperature for at least 48 hours prior to use. A summary of the properties of these compounds is presented (Table 1).

Table 1. Properties of polyurethane components.

Property	Material			
	MDI	HPC	HPL	CPL
Isocyanate equivalent weight	133			
NCO content, %	31.5			
Viscosity at 25°C	250cps			
Specific gravity	1.23	1.15	--	1.07
Hydroxyl content, %		15.8	9.5	--
Hydroxyl number, mg KOH/gm				310
Molar substitution	--	3.27	--	--

3.2 METHODS

3.2.1 Resin Preparation

The calculated amount of HPC, typically 2-3.5 g, was dissolved in 25 mls of THF, with mechanical stirring. The stoichiometric amount of MDI was added with further stirring, and allowed to stay for at least 5 minutes. The resin is then degassed prior to DMTA sample preparation. HPL-based resins were prepared in a similar fashion except that excess amount of THF, typically 35 mls for 2- 3.5 g of HPL, was used to avoid gelation while mixing the various components. Caprolactone triol-based resins were prepared without THF. The formulation and/or calculation of the composition of the various resins is presented (Table 2).

3.2.2 DMTA Samples Preparation

A suitable method to perform dynamic mechanical analysis on thermosetting systems undergoing cure is by the use of glass fiber braid as a support for the reaction mixture which is initially a liquid at the temperature of cure. In the first section of this study, reaction kinetics, glass fiber braids of approximately 12 x 25 mm in dimension were submerged in the reaction mixture with the excess being wiped off with a glass rod. The ends of the samples were covered with aluminum foil to avoid contact between the reaction mixture and the DMTA clamps. Samples for vitrification and damping behavior were prepared differently from the above as described below.

Table 2. Formulation of polyurethanes.

Designation	Polyol component wt. fraction, %	Isocyanate wt. fraction, %	NCO/OH Ratio
HPC ¹	44	56	1.5
HPL ¹	40	60	1.5
CPL ¹	35	65	1.0
HPL ²	70	30	0.8
HPL ³	55	45	0.8 - 2.5

¹ Samples for cure kinetics study.

² Samples for vitrification study.

³ Samples for damping behavior study.

The resin was poured on steel plates coated with a thin layer of silicone oil and allowed to stand for 3-5 minutes at room temperature in a hood to evaporate the solvent and set in the form of a uniform film. The films were cut into pieces, with typical dimensions of 8 x 12 mm.

Cure of these films was carried out in a vacuum oven for periods ranging from 5 minutes to 16 hours at temperatures of 45°C to 100°C.

3.2.3 Product Analysis and Testing

The DMTA, including the bending head and the universal temperature programmer, used in this study were manufactured by Polymer Laboratories. Data were collected using a PL Plus V software and stored in PL binary format, which were later converted to PL ASCII for print out. The mode of operation and/or the theoretical principles of the DMTA has been described elsewhere.⁴³

Bending of samples, in the kinetic study, was carried in a double cantilever mode, at a heating rate of 2.5°C/minute. An 0.4 mm oscillation amplitude was used in all runs. A nitrogen purge at a rate of 25 cc/min was used during data collection. The DMTA kinetic study consisted of isothermal and dynamic temperature scanning. Each isothermal run consisted of three steps. The first step gives the isothermal cure behavior; the second step involved a dynamic temperature scan and gives the T_g of the partially-cured material and completes the residual cure. The final step, which also involved a dynamic temperature scan, gives the thermomechanical behavior of the fully-cured material. All DMTA runs were carried out at a frequency of 1 Hz.

Samples for vitrification and damping behavior studies were cured in a vacuum oven and withdrawn for the determination of the T_g , via DMTA, attained after each cure schedule. Heating rates, oscillation amplitude, and frequency were similar to those mentioned previously.

CHAPTER 4

4.0 RESULTS AND DISCUSSION

4.1 MODEL CONSIDERATIONS

In order to assess the relative reactivity of the various wood components with isocyanate, it becomes necessary to dissolve them in a suitable solvent prior to mixing with isocyanate. However, due to the insoluble nature of wood components, particularly cellulose and hemicellulose, model wood components were used (see Chapter 3). It was impossible to dissolve hydroxylpropyl xylan, a model of hemicellulose, in the solvent used.

HPC, and in general, cellulose derivatives form a phase of intermediate order which arises as a consequence of liquid crystal mesophase formation during solvent evaporation.³⁸ The consequence of such a phenomenon is making hydroxyl groups less accessible to other reactive groups. This situation might be parallel to the inaccessibility of hydroxyl groups in native cellulose, i.e. that present in wood. However, the close association of cellulose molecules, and with other wood components, would induce restricted mobility in cellulose segments in wood compared to HPC. This same restricted mobility could be said of lignin. Furthermore, the un-derivatised hydroxyl groups in lignin are more reactive than

those present in HPL. Thus, it is recognized that cellulose and lignin would behave to some extent, differently from these model compounds. Nevertheless, the reactivity of these model compounds, and water with isocyanate, might provide some information on the dominating reaction during wood bonding with isocyanate.

It should be emphasized that hemicellulose has a blend of the characteristics of lignin (branched) and cellulose (linear), and should accordingly have an intermediary reactivity of the two.

The discussion of

- a) The relative reactivity of wood components and moisture with isocyanate is based on kinetic study analysis, via DMTA, of model materials with isocyanate in solution, and the visual observation of the reaction of water with isocyanate. No quantitative kinetic results could be made of the latter reaction, since it was very fast, making it impossible to prepare samples.
- b) Vitrification behavior of the polyurethanes is based on samples which are partially-cured in a vacuum oven and withdrawn for T_g determination via DMTA.
- c) The effect of resin stoichiometry on network formation is based on HPL-based polyurethanes at various molar ratio of isocyanate (NCO) to hydroxyl (OH), subjected to multi-frequency dynamic mechanical thermal analysis.

4.2 TEMPERATURE SCAN OF RESINS

In order to evaluate the thermal behavior of the resin, a temperature scan was made from -60°C to 300°C . The cure spectrum for an HPL-based resin is presented (Figure 9). The storage modulus drops steeply and goes through a minimum at 25°C , and thereafter shows a steep rise prior to 84°C . Beyond 84°C , there is a gradual rise before finally levelling off near 300°C . Three maximum peaks were observed in the loss modulus at -15°C , 84°C and 164°C .

The storage modulus of the HPC-based resin shows a similar decreasing trend, as was the case for the HPL-based ones; however, the minimum peak occurred at a slightly higher temperature and the steep rise in storage modulus thereafter is continuous to about 240°C , and drops again. The loss modulus displays only two transitions, at -17°C and 118°C (Figure 10).

The first maximum in the loss modulus, at -15°C and -17°C for HPL- and HPC-based resin, respectively, (Table 3) is displayed as the resin goes through its glass transition. Since the resin is without crosslinks, the low transition temperature was expected. This temperature is designated as T_{g0} , the glass transition of the uncured resin, in the TTT cure diagram,¹⁵⁻¹⁷ and is considered as the maximum safe storage temperature to avoid precure or for long-term stability.

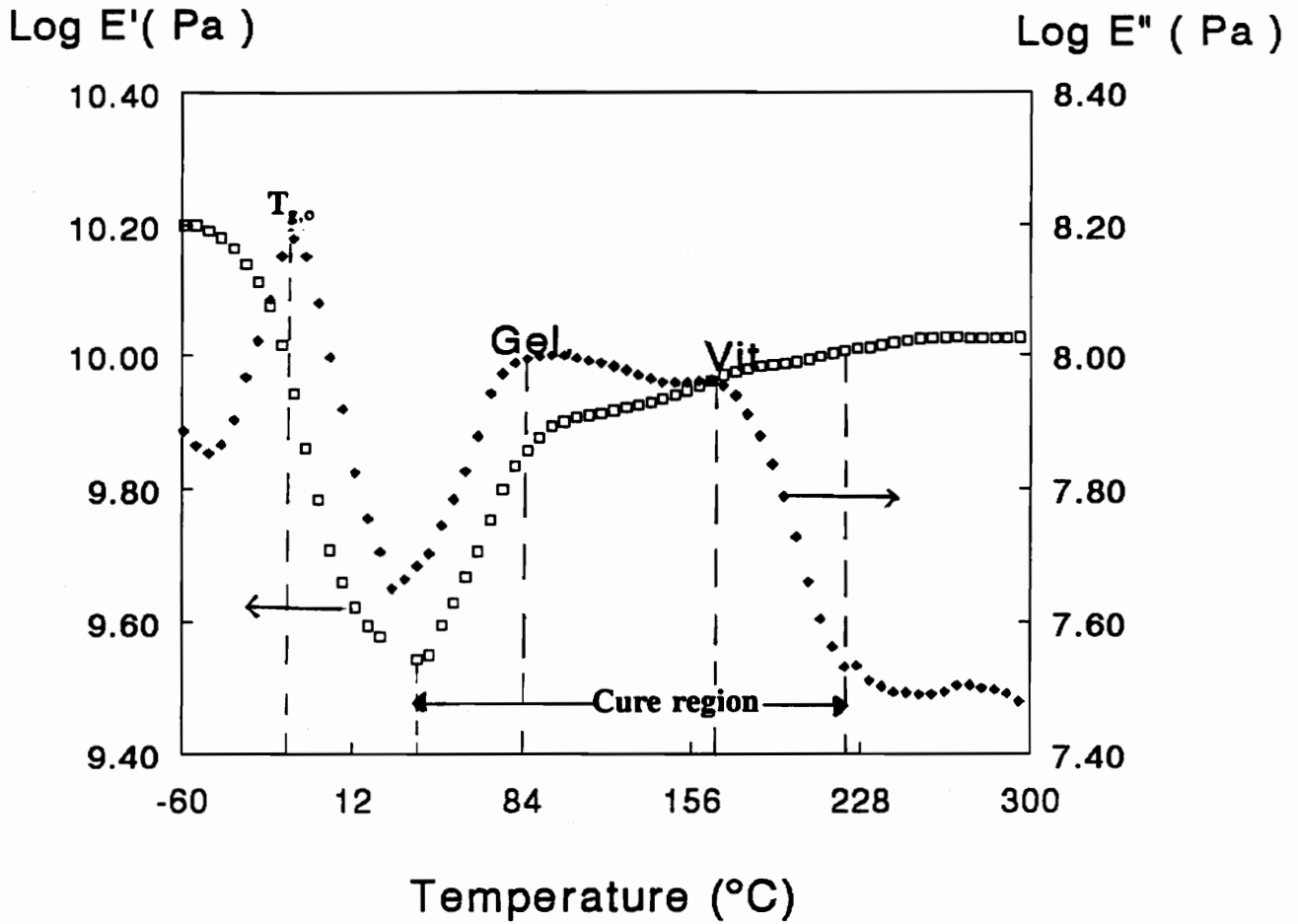


Figure 9. A temperature scan profile of HPL-based resin. Cure of this resin starts at 30°C and proceeds at fast rate to 164°C, the temperature at which vitrification occurs. The cure rate beyond vitrification is considerably slowed down.

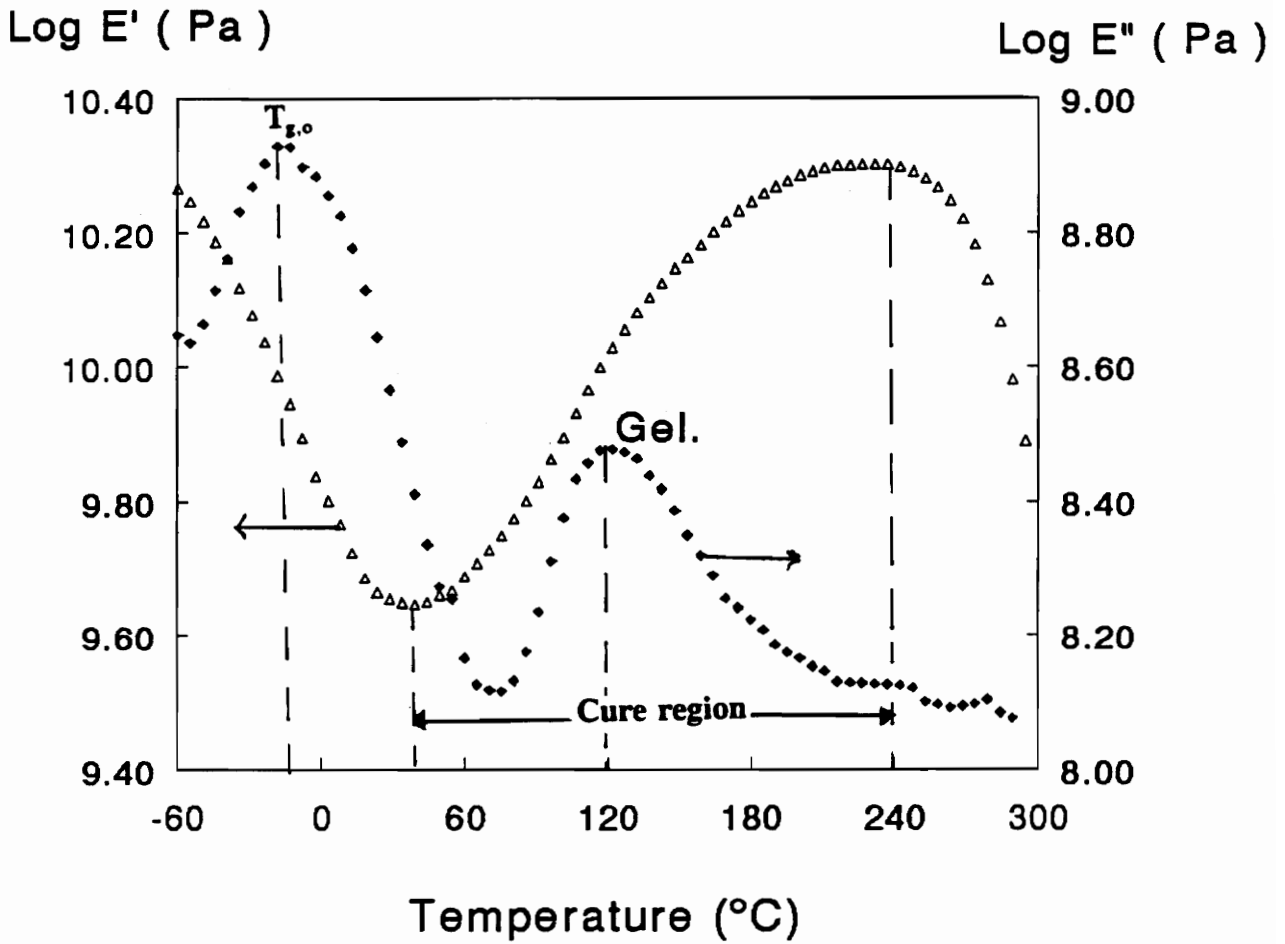


Figure 10. A temperature scan profile of HPC-based resin. Cure of this resin starts at 40°C, beyond which thermal degradation takes over. No vitrification peak is seen in the cure profile of this resin.

Table 3. The temperature of vitrification and gelation, and the glass transition temperature of the uncured resin.

Resin	T_{go} (°C)	T_{gel} (°C)	T_{vit} (°C)
HPC-based resin	-15	118	--*
HPL-based resin	-17	84	164

T_{go} : glass transition temperature of uncured resin

T_{gel} : temperature of gelation

T_{vit} : temperature of vitrification

* No transition characteristic of vitrification.

The maximum peaks at 84°C and 118°C for HPL- and HPC-based resin, respectively, are due to gelation of the resin, and that at 164°C for HPL-based resin is due to vitrification (Table 3). At the initial stage of cure, damping is low since the resin is in the liquid state. Damping increases, however, as the resin becomes more rubber-like, but decreases beyond the gel point since increasing crosslinks restrict molecular mobility. Damping exhibits a second maximum as the network transforms from the rubbery to the glassy state, in an analogous fashion to the glass to rubber transition, and serve as a basis for identifying the loss modulus peaks, at the mentioned temperatures as due to gelation and vitrification.

The fact that no vitrification peak was observed for the HPC-based resin should not be a basis to say that the cure of this system proceed, only to a rubbery state. In fact, physical examination of the cured materials indicated that they are glassy. A plausible explanation for the absence of a vitrification peak is that thermal degradation predominates over cure beyond 240°C, and precludes any damping maximum that could otherwise be identified with additional cure.

The initial drop in the storage modulus is attributed to the relaxation process accompanying the low-temperature transition, and thermal softening of the resin. Above 30°C, however, the drive towards cure overcomes these two events, with a corresponding minimum in the storage modulus.

The gradual rise in the storage modulus following vitrification of the HPL-based resin was not surprising. Following vitrification, the reaction proceeds in the

glassy state and is diffusion-controlled. Consequently, the reaction is slowed down considerably.

No temperature scan assessment could be made of the resin from caprolactone triol and MDI since it gelled immediately after mixing of the components.

The practical significance of this is, in using these resin systems in bonding applications where sufficient spread and/or flow of resin is essential, the bio-based resins offer a better option than the caprolactone-based resin. The latter might gel immediately on application to the bonding surface, precluding sufficient spread.

4.3 ISOTHERMAL CURE OF RESINS

Examples for isothermal cure monitoring spectra for HPC-based resins are shown (Figure 11 a & b). The absolute value of the modulus is not representative of the resins' modulus since it is that of a composite. Nevertheless, the rise of modulus is due to changes in the modulus of the polymer phase since the glass fiber braid exhibit a constant modulus over the entire cure period.¹⁴ No maximum, typical of gelation and vitrification, is seen in the loss tangent for cure temperatures ranging from 30°C to 190°C (e.g., Figures 11 a & b). It is speculated that vitrification of the system studied should occur beyond the isothermal cure time. The absence of a

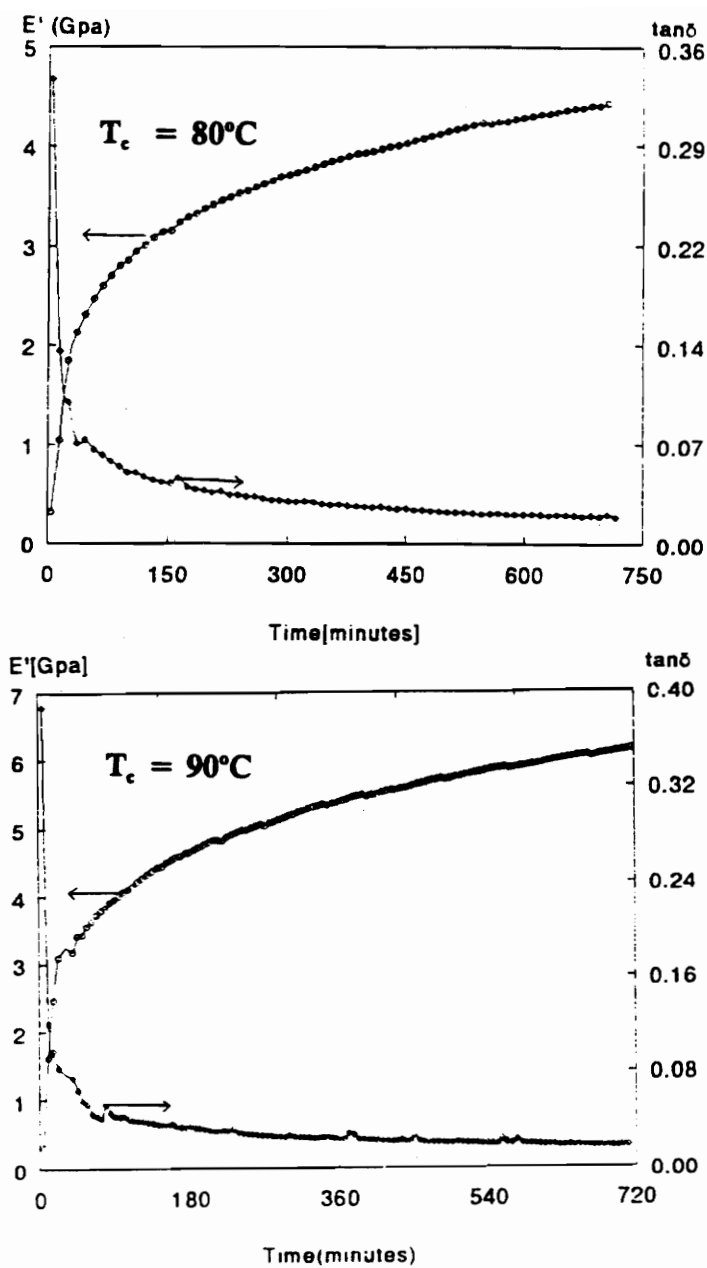


Figure 11 a&b. Isothermal cure profile of HPC-based resins at two cure temperatures. The $\tan \delta$ trace do not display transitions typical of gelation and vitrification.

gelation peak is, however, very surprising since the same material gave such a distinctive peak in the dynamic temperature scan.

Hofmann^{19,20} and Zumburum⁵⁰ have reported a similar absence of vitrification and gelation peaks in cure monitoring of lignin-based epoxy and acrylate resins, respectively, via DMTA.

An attempt was made to use the cross-over of the storage and loss moduli (E' and E'' , respectively), as an indication of the gel point.⁷ However, no cross-over of the moduli occurred, the storage modulus was higher than the loss modulus over the entire cure time (Figure 12).

Connolly and Tobias¹⁰ made a parallel observation during cure studies of polyester prepregs. However, there are reported cases of the crossover of the two moduli, for resins studied in neat bulk form.⁷ The system studied, and those of Connolly and Tobias, are highly reinforced; it is, therefore, assumed that this criterion in the form of E' and E'' cross-over is applicable to neat/bulk systems only.

Following cure, the partially cured samples were controlled cooled to subambient temperature to preclude possible aging, and probe, in a dynamic mode to obtain the T_g attained under each isothermal cure. A summary representation of the T_g attained after twelve hours of cure at various temperatures is shown (Figure 13) where T_g is plotted against cure temperature. The linear rise of T_g with cure temperature is reasonable. In the absence of thermal degradation, high temperatures promote much crosslinking with its associated high T_g s.

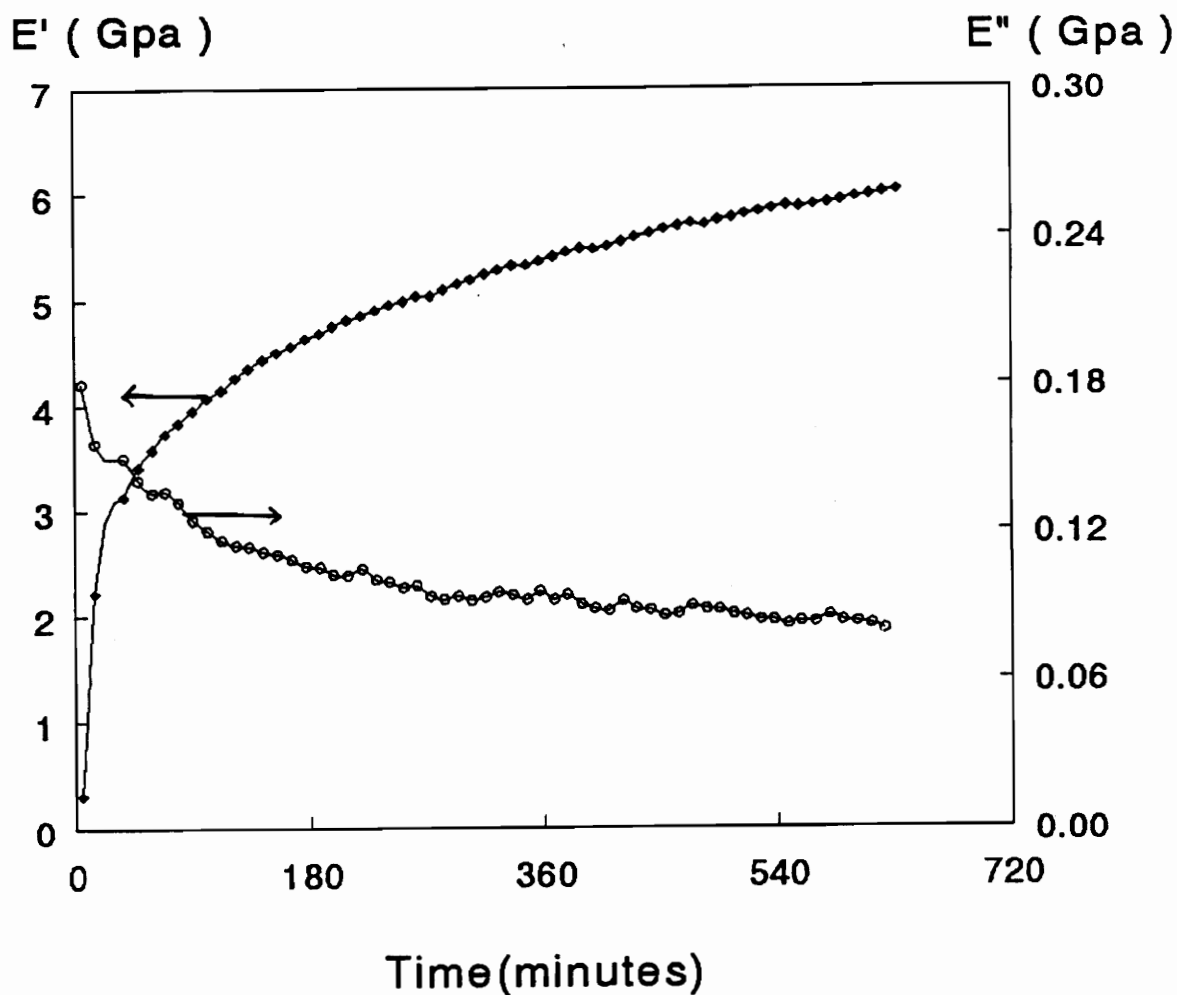


Figure 12. An illustration of nonconformity to the criterion of using E' and E'' crossover as gelation in the HPC-based polyurethanes. The two curves tend to crossover only because they are not on the same scale.

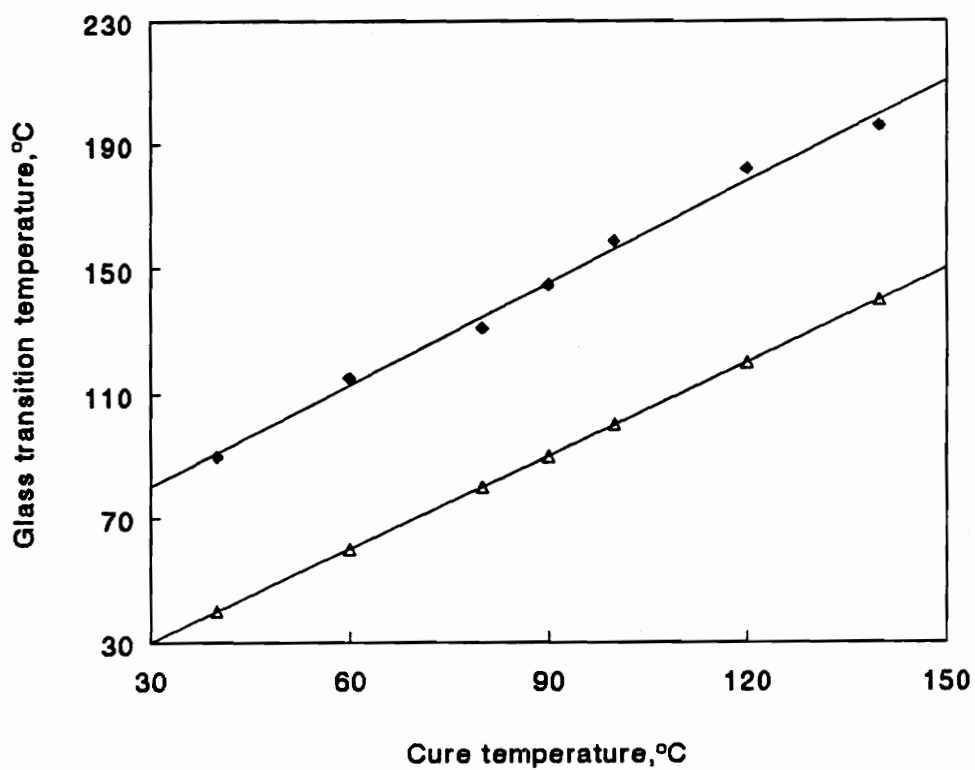


Figure 13. Glass transition temperature of HPC- and HPL-based polyurethanes versus cure temperature. The upper curve represents T_g s obtained after twelve hours of cure at various cure temperatures, and the lower curve represents a theoretical consideration, i.e. where $T_g = T_c$.

The HPC-based polyurethane displayed two transitions; a lower transition temperature at 30° - 44°C and a high transition at 90°C to 210°C depending on the cure temperature (Figure 14). Rials and Glasser^{38,39} have made a similar observation in HPC crosslinked with TDI, and have attributed the low and high transitions to an amorphous and crystalline phase in HPC, respectively.

The observed glass transition temperatures were higher than the cure temperatures (Figure 13), and considering the definition assigned to vitrification, where T_g becomes equal to T_c , it is surprising that no vitrification peaks were seen in the isotherms.

Gillham et al.¹⁶⁻¹⁸ have proposed an explanation for the fact that the observed T_g following isothermal cure to vitrification is higher than T_c as follows:

- the temperature scan for T_g determination can promote further reaction;
- isothermal cure is carried out well beyond the vitrification peak, where reaction is assumed to cease. However, reactions can proceed in the glassy state to an appreciable extent.

Whereas these explanations could be applicable to the observed T_{gs} of the polyurethane studied, it should be recognized that a cellulose backbone, with a characteristic stiff chains would undoubtedly result in high T_{gs} .

A puzzling behavior of the HPC-based polyurethane is that the T_{gs} for isothermal cure times from 1 to 12 hours at a particular temperature are identical

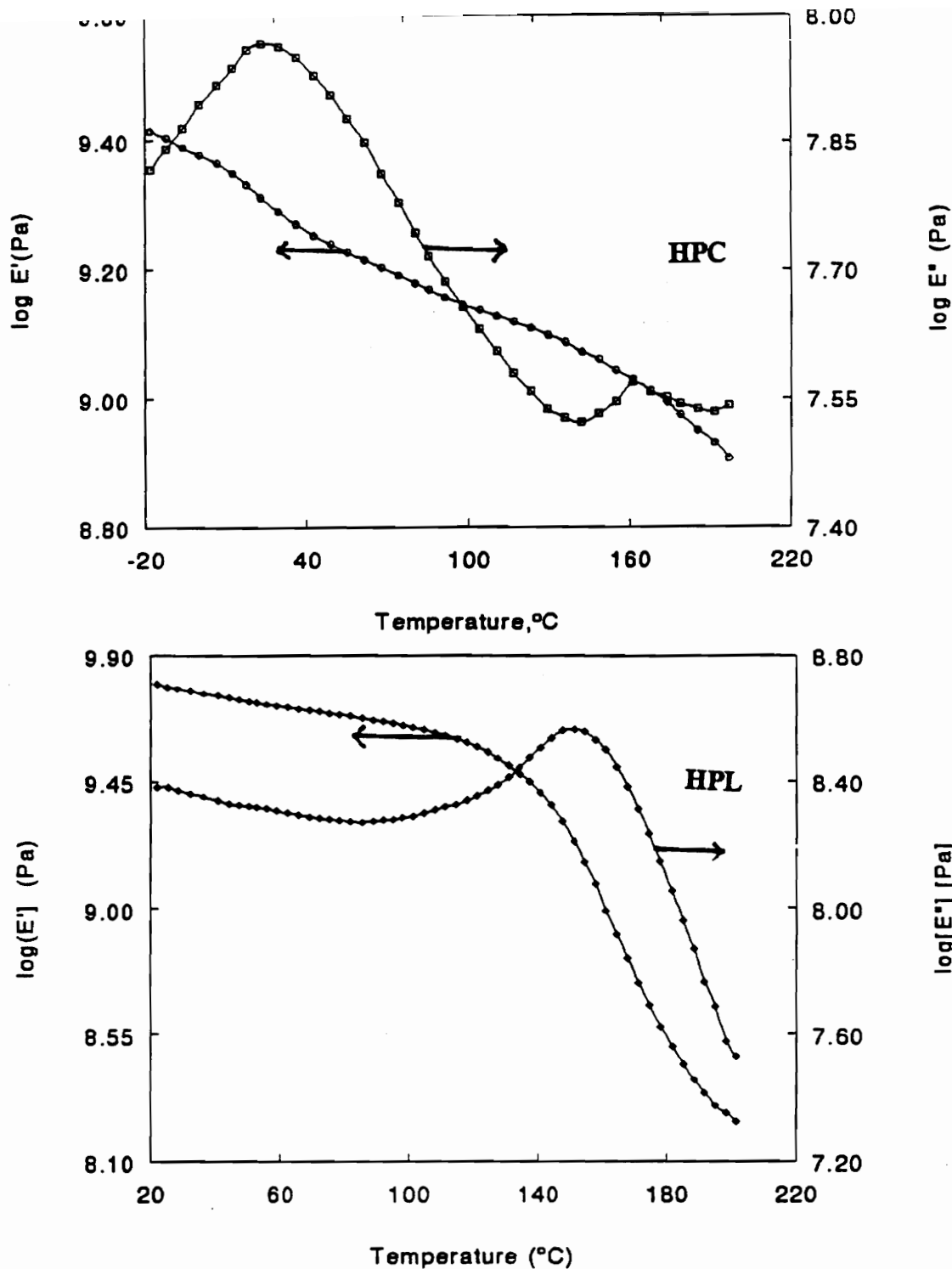


Figure 14. Characteristic transitions displayed by HPC- and HPL-based polyurethanes cured at 100°C for twelve hours. The higher initial storage modulus (E') of the HPL-based polyurethane is a result of differences in the logk factor used in the DMTA, and does indicate that HPL-based polyurethane is stiffer at low temperatures than HPC-based polyurethane.

(Figure 15). This behavior can only be accounted for by two effects:

- (1) additional crosslinking arising from side reactions; allophanate formation;
- (2) the polymer chains might have been frozen in position and consequently freezing the cure process. Relaxation of such chains during the temperature scan might have promoted further molecular entanglement to affect additional crosslinking.

One would expect that if (1) and (2) are reasonable explanations, they should affect an appreciable increase of storage modulus and damping, respectively. However, DMTA is less sensitive to modulus rise measurement towards the end of cure hence the slight increase of E' . Additional polymer chain entanglement tends to restrict mobility of the polymer chains, and invariably dominated any damping rise that would have accompanied effect (2).

No isothermal cure monitoring of HPL-based resin is reported in this study. This is because when this resin was subjected to isothermal cure, it was found that, by the time the sample attained the necessary cure temperature, a significant portion of the reaction had occurred, such that the modulus is essentially flat thereafter.

A dynamic scan profile of fully-cured HPL-based polyurethanes reveals different features than those of HPC-based polyurethanes (Figure 14).

Only one transition with a characteristic high amplitude at 90°C - 160°C , depending on the cure temperature, is displayed by the former. The latter, on the

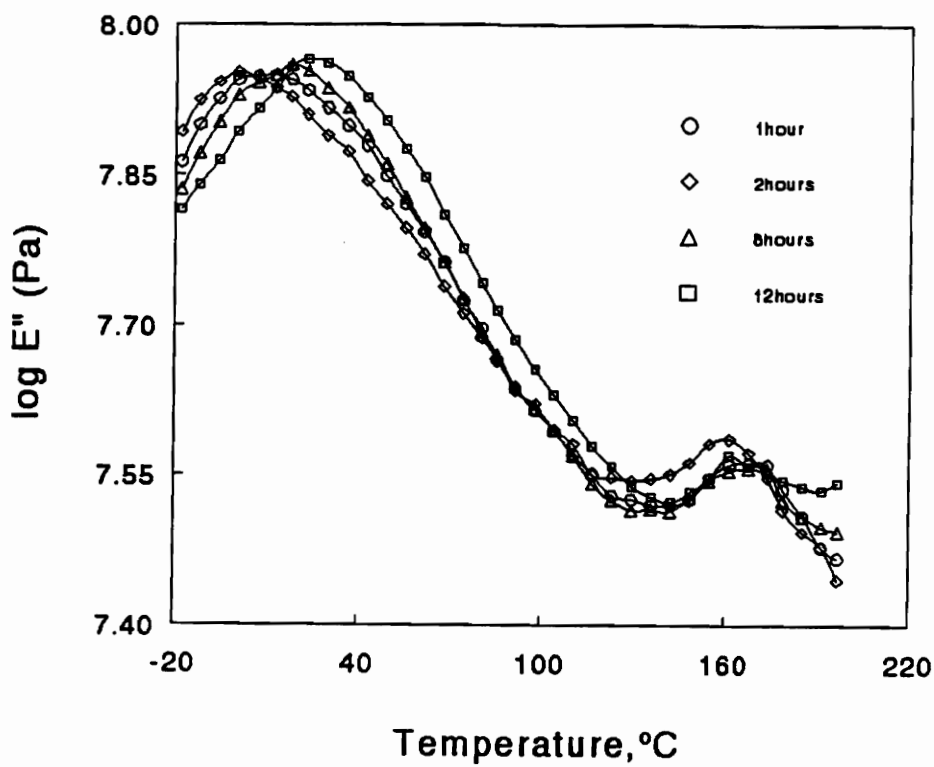


Figure 15. Comparison of T_g of HPC-based polyurethanes for various isothermal cure times at T_c of 90°C. The T_g s lie in the range of 160°C to 165°C.

other hand, displays two transitions and has been attributed to the fact that HPC consists of two phases. The transition, at 30°C-44°C, due to the amorphous regions of HPC has amplitude comparable to that of HPL.

These results indicate that HPL consist of only one phase, amorphous regions, and that these regions enhance damping in the bio-based polymers. Furthermore, the storage modulus (E') trace of HPL-based polyurethanes show a marked decline as opposed to that of HPC-based polyurethanes, which besides a gradual decline show a slight increase near 100°C-120°C, due to the side reactions explained previously. This result suggests that the incorporation of flexible polyether segments, i.e. the derivatization of cellulose to molar substitution of 3.27, did not sufficiently increase the mobility and/or flexibility of the cellulose segments. Another explanation for the retention of stiffness in HPC-based polyurethane could be sought in the fact that HPC form crystalline regions, as explained previously, thus improving its stiffness.

In practical terms, it could be recognized that in applications where retention of stiffness at low to medium temperatures, say between 100 and 220°C, is necessary, HPC-based polyurethanes offer a better option at the mentioned molar substitution over their HPL-based counterparts. On the other hand, where good damping behavior matters, such as in polymers for vibration or noise reduction, the latter is a better choice.

4.4 KINETICS OF HPC AND HPL CROSSLINKING WITH ISOCYANATE

The storage modulus profile for HPC- and HPL-based resins (Figures 9 and 10) were subjected to an n^{th} order kinetic analysis according to the procedure proposed by Provder et al.³⁴ outlined in Section 2.2.2. Fractional cure (F) was obtained in the temperature range 44°C - 215°C and 70°C - 227°C for HPL and HPC, respectively, at intervals of 20°C, according to equation (2.20). The rate of cure with temperature (dF/dT) were computed using equation (2.22) and a series of rate constant (k) at various temperatures were computed from equation (2.24), assuming orders of reaction of 1.5, 1.8, 2.0, and 2.2.

The appropriate order of reaction was selected by evaluating the linearity of the Arrhenius plot $\ln k(T)$ versus $1/T$ (Figures 16 a & b). The order of reaction that gave the best fit was 1.8 ($R^2 = .98$). The reaction of isocyanate with hydroxyl compounds has been reported to follow second order kinetics,^{6,29,34,48} therefore the 1.8 value obtained in this study is reasonable.

The activation energy of the cure reaction, obtained from the slope of the Arrhenius plot, is compared with that obtained in other studies (Table 4). It should be emphasized that however close the activation energy obtained in this study is to that reported in the literature, it is an apparent kinetic parameter since it describes a chemorheological process in which a purely chemical mechanistic interpretation of the parameter is not valid.

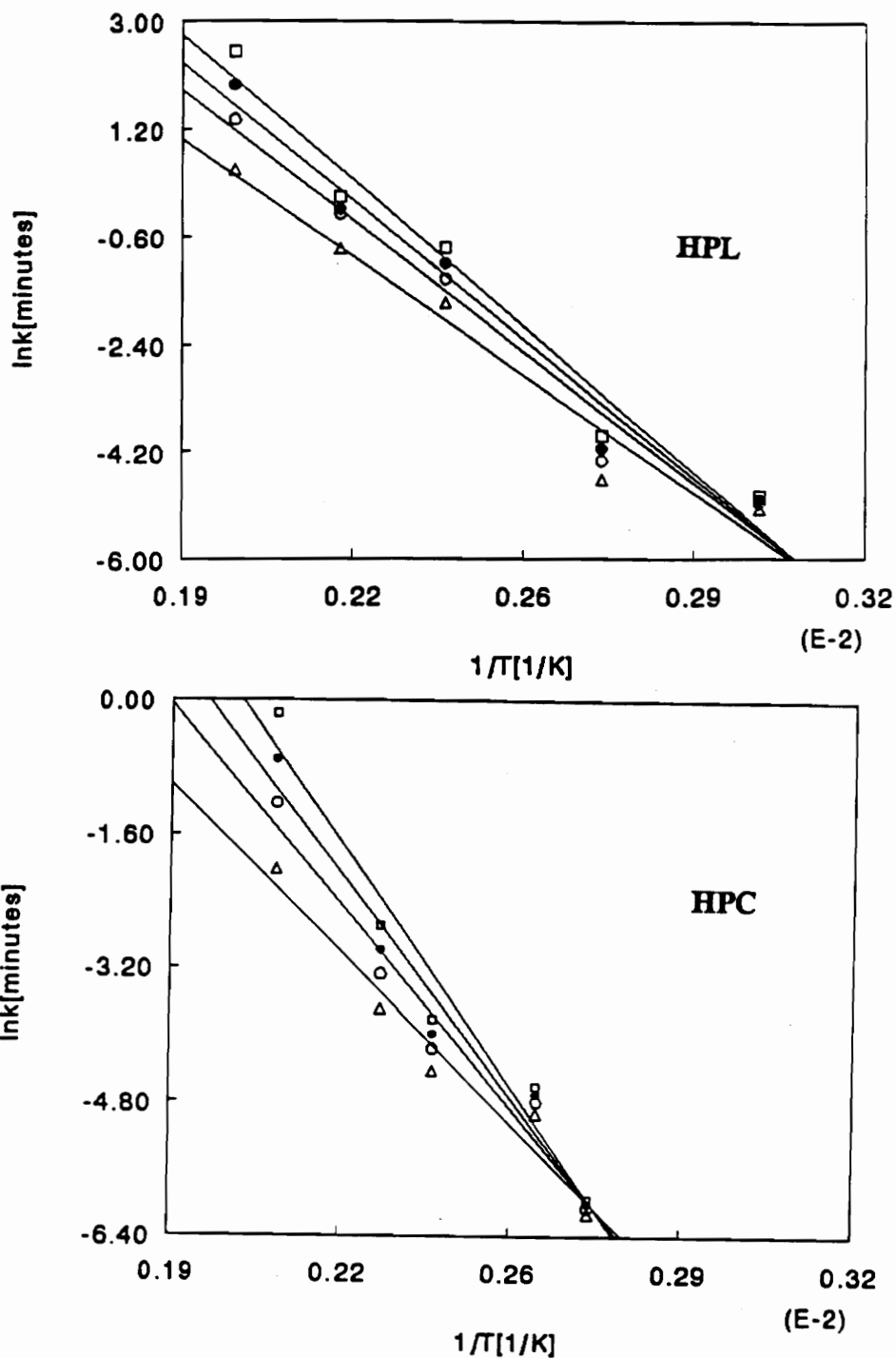


Figure 16 a&b.

Arrhenius plots of $\ln k$ versus reciprocal temperature. The slope of the various lines is used to compute the activation energy of the cure reaction according to equation 2.23. The n^{th} value that gave the highest correlation coefficient was 1.8 ($R^2 = .98$) and is taken as the order of reaction of these bio-based polyurethanes.

Table 4. Comparison of activation energy of polyurethane cure.

E_A (kcal/mol)	S_m	n	System	Reference
14.7	dmta	1.8	HPC/MDI**	this work
16.5	Viscosity measurement	2*	PCPL/MDI**	29
9.5	FTIR	2*	HEA/HDI**	4
8.2	FTIR	2*	HPO/TIP**	12

* assumed value

** in solution

S_m study method

n order of reaction

E_A activation energy

PCPL polycaprolactone triol

MDI methylene diphenyl diisocyanate

HEA hydroxyethyl acrylate

HDI hexamethylene diisocyanate

HPO dihydroxypoly (propylene oxide)

TIP tris (4-isocyanatophenyl thiophosphate)

In deriving fractional cure, the maximum in the storage modulus at 240°C and 300°C for HPC-based and HPL-based resins was assumed as the final modulus of the fully-cured polymer. The validity of the above assumption is limited, particularly in the case of the HPC-based polymers. In the absence of thermal degradation beyond 240°C, additional cure might have occurred.

Notwithstanding the above uncertainty, the activation energy and pre-Arrhenius factor obtained have been used to compute the degree of cure (F) and rate of cure with time ($[d(F)]/dt$) at two temperatures according to equations (2.20) and (2.22), respectively (Figures 17 a & b).

The degree of cure was higher in the HPL-based polymers than their HPC-based counterparts. This trend stems from the fact that the hydroxyl groups in HPC are less accessible to isocyanate as opposed to those of HPL. The cause of inaccessibility of the hydroxyl groups in HPC has been explained in section 4.1.

The rate of cure with time followed a parallel trend at the initial stages of cure. The difference vanished in the latter stages, indicating that the effect of differences in the accessibility of hydroxyl groups on cure rate is significant only in the early stages.

The rate of cure with temperature derived from Figures 9 and 10, according to equation (2.20) is also presented (Figure 18). Both HPL- and HPC-based polymers show an increasing trend of cure rate prior to gelation, 84°C and 118°C, respectively (Figure 18 a). The latter, however, shows only a decreasing trend

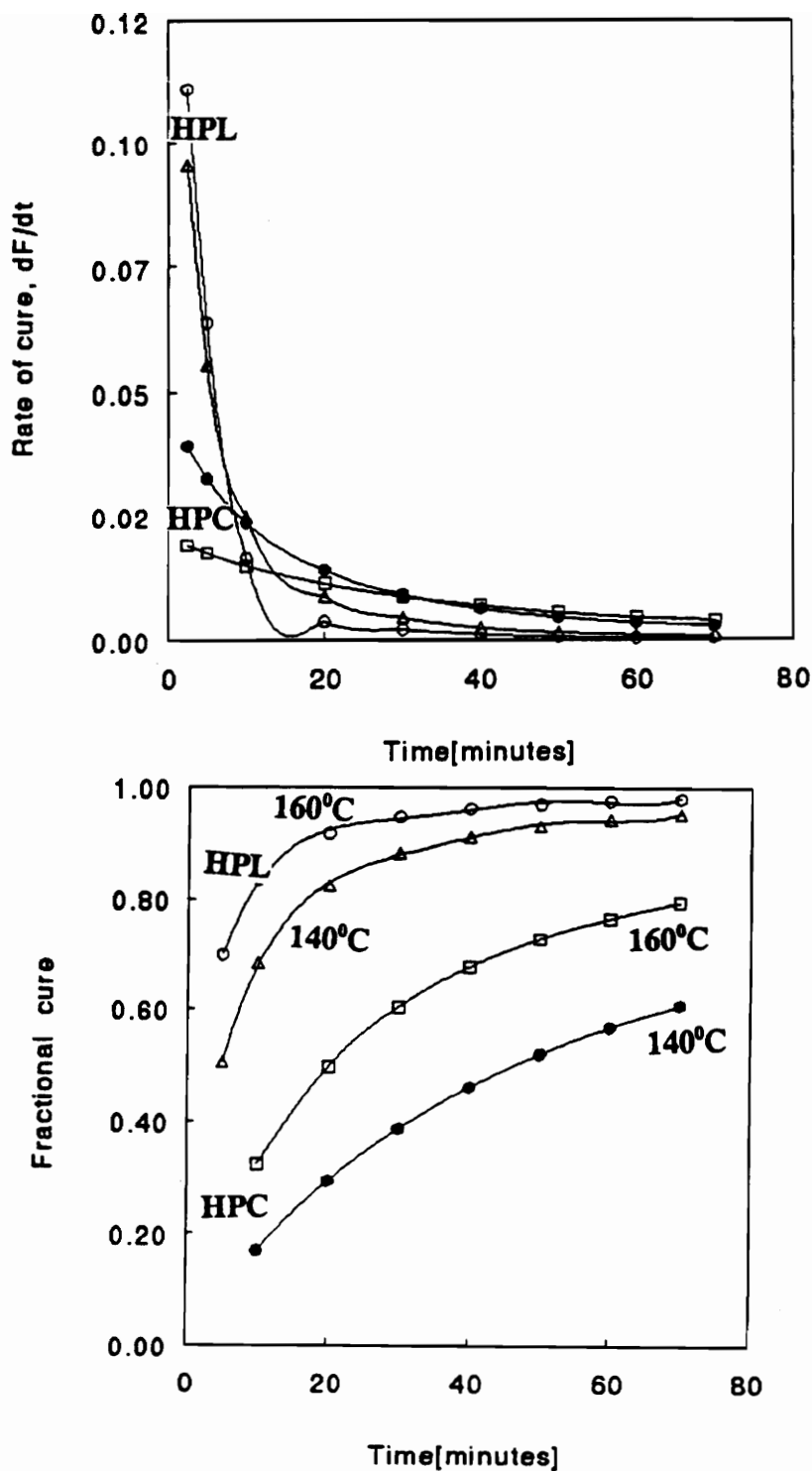


Figure 17 a&b.

Rate of cure and degree of cure in HPC and HPL-based resins. The difference in the rate of cure between HPC- and HPL-based polyurethanes vanishes under twenty minutes and might indicate the influence of diffusion limitations on cure.

beyond gelation, while the former shows an increasing trend at 135°C to 169°C, and thereafter decreases. The decreasing trend immediately after gelation indicates that the rate of cure is impaired by gelation. The temperature at which the second increasing trend is observed for the HPL-based polymers is within the vicinity of vitrification, marking the transition from the rubbery to glassy state. This should be associated with enhanced crosslinking. The one-step increase of rate of cure with temperature in HPC-based polyurethanes has its roots in the absence of vitrification, and its attendant additional crosslinking. The decreasing trend beyond 169°C is expected, since after vitrification the reaction proceeds in the glassy state and thus slowed down considerably.

An attempt was made to study the kinetics of isocyanate crosslinking with caprolactone triol; however, this effort was futile. It was observed that gelation of the resin, occurred immediately following mixing of the components, indicating a much higher rate of cure.

The kinetic parameters obtained in the previous procedure were compared with those obtained in isothermal cure experiments (Table 5) and described below. Isothermal cure profiles (e.g., Figure 11 a & b) for different cure temperatures were subjected to an n^{th} order rate expression, deriving fractional cure from the isotherms in a similar fashion as done in the previous approach.

The integral form of equation (2.22) was used to examine the kinetics of the cure reaction as follows:

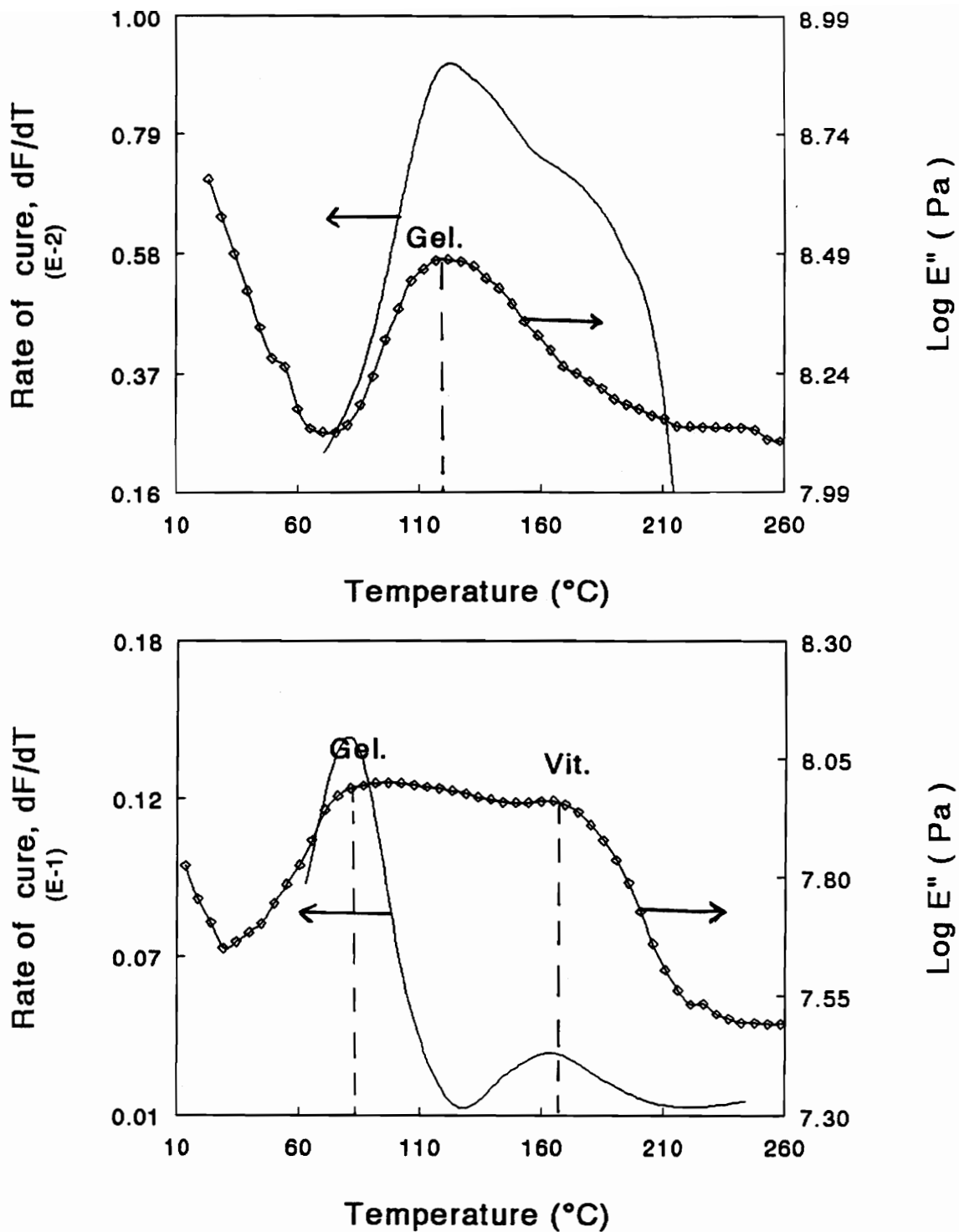


Figure 18. Rate of cure with temperature in HPC and HPL-based resins. A trace of the loss modulus (E'') displayed in dynamic cure is indicated to illustrate the effect of gelation and vitrification on cure rate.

Table 5. Isothermal and dynamic kinetic cure parameters.

System	E_A (kcal/mol)	$\ln A$ (min^{-1})	n
HPC/MDI ¹	14.7	14.1	1.8
HPC/MDI ²	13.0	11.9	1.8
HPL/MDI ¹	13.4	14.7	1.8

¹ dynamic kinetics.

² isothermal kinetics.

A pre-Arrhenius factor.

$$\left[\frac{1}{1-n} \right] \left[[1-F]^{1-n} - 1 \right] = k(T)t \quad n \neq 1 \quad (4.1)$$

where n , f , and k have their usual meaning.

By plotting the left-hand side of the above equation, assuming values for n , as a function of time, a straight line indicates the reaction order and the slope gives the reaction rate constant $k(T)$. However, based on the fact that the apparent activation energy from the previous approach using $n = 1.8$ compared favorably with literature values, the same value was assumed in this case. Plots of the rate expression, as a function of time, at various cure temperatures are presented (Figure 19). The slopes yield rate constants at the various cure temperatures. These rate constants were plotted against temperature, in Arrhenius form (Figure 20) to obtain the apparent activation energy and pre-Arrhenius factor (listed in Table 5), according to equation (2.23).

Fractional cure at 100°C and 140°C is predicted using equation (2.26) and compared with measured values (Figure 21). The lines shown have nearly identical slope, thus the model equation and 1.8th order are acceptable.

An isothermal kinetic analysis of HPL-based polymers was not possible. It was observed that by the time the DMTA attained cure temperature (i.e., 60°C-160°C), a significant portion of the cure reaction had occurred, and hence a flat modulus profile was observed thereafter. A comparison of the kinetic cure parameters, activation energy and pre-Arrhenius factor (Table 4), indicate that they

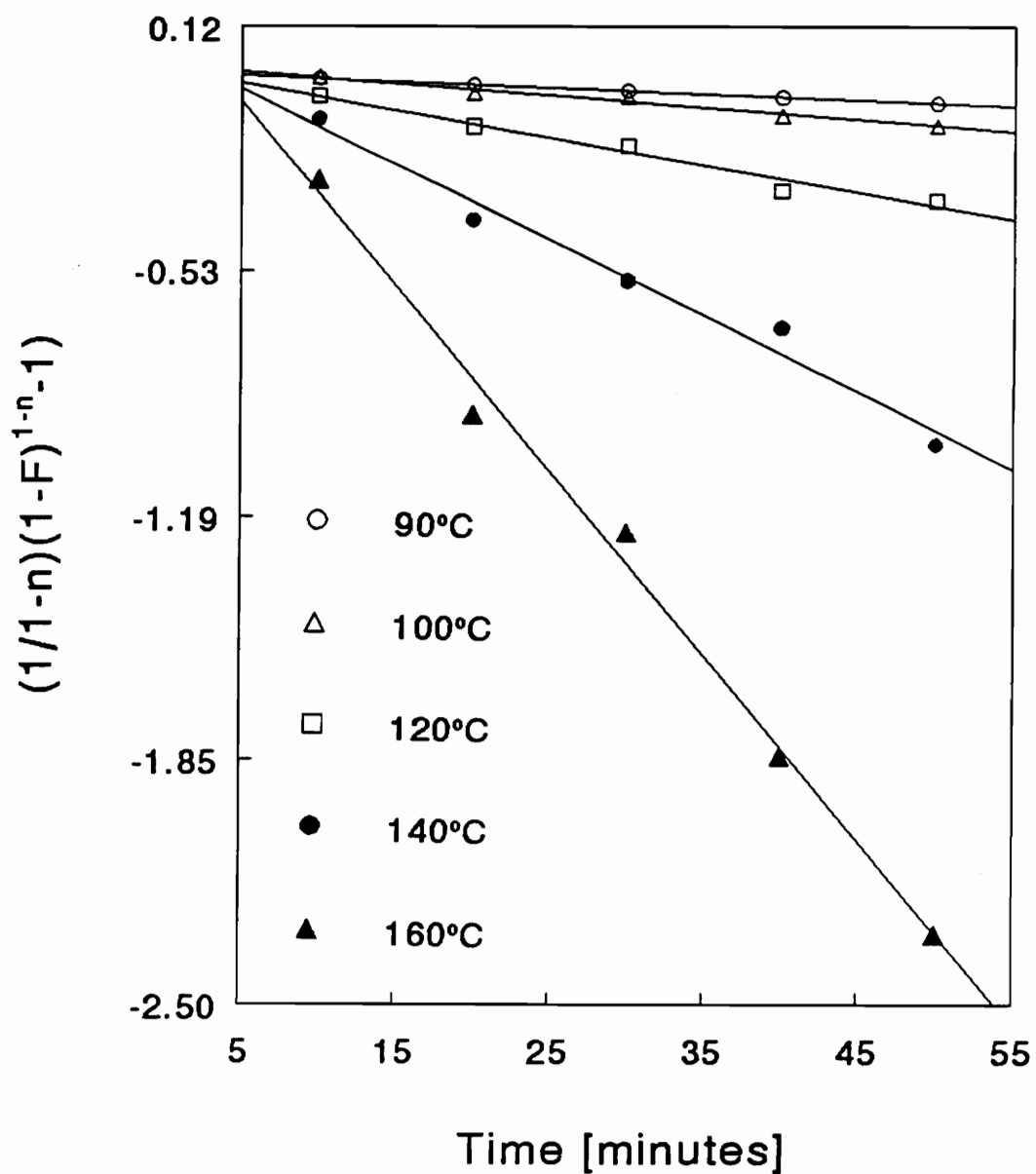


Figure 19. Rate expression versus time for the determination of rate constants at various cure temperatures for HPC-based polyurethane. The rate constant, k , at each cure temperature is obtained from the slope of the curves according to equation 2.25.

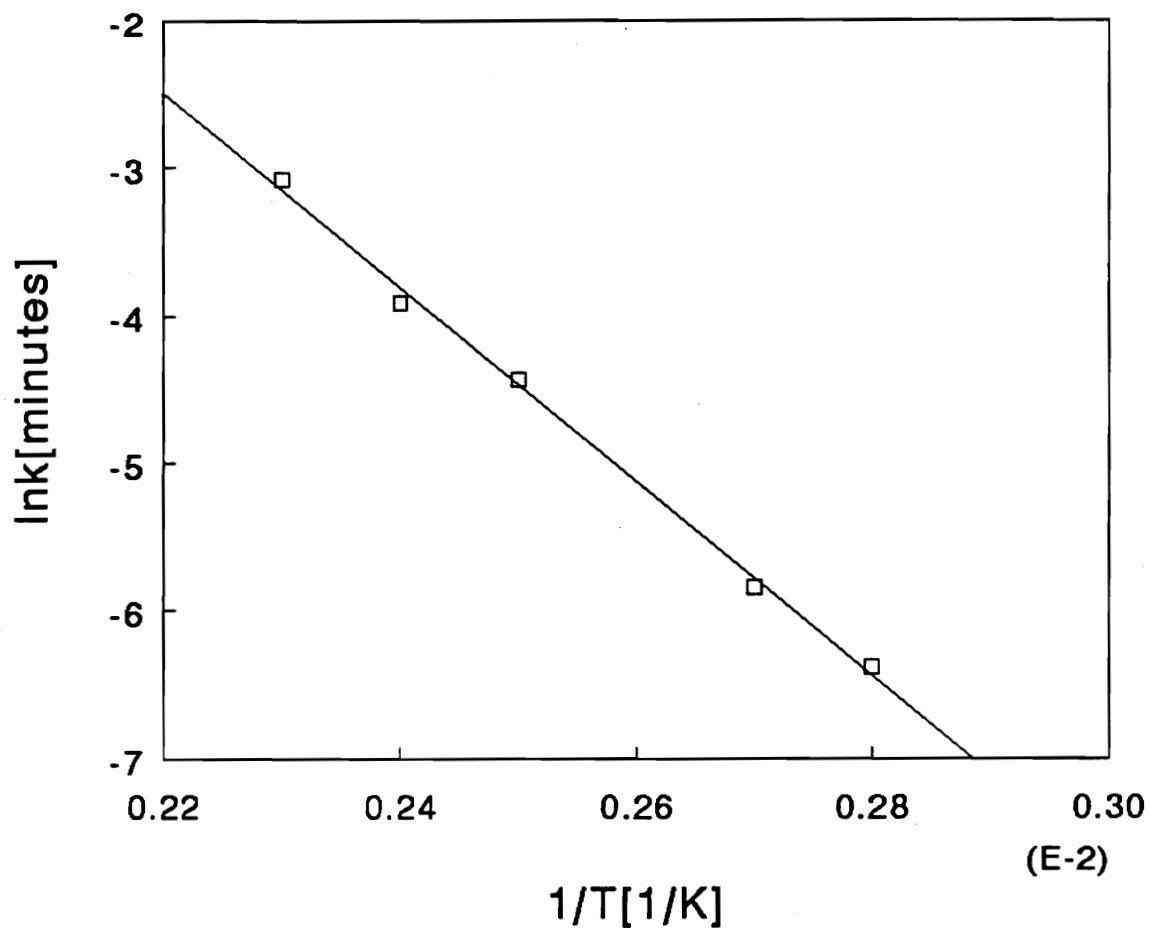


Figure 20. Arrhenius plot of rate constant versus temperature for activation energy determination of HPC-based polyurethanes. The activation energy of cure is determined from the slope of the curve according to equation 2.23.

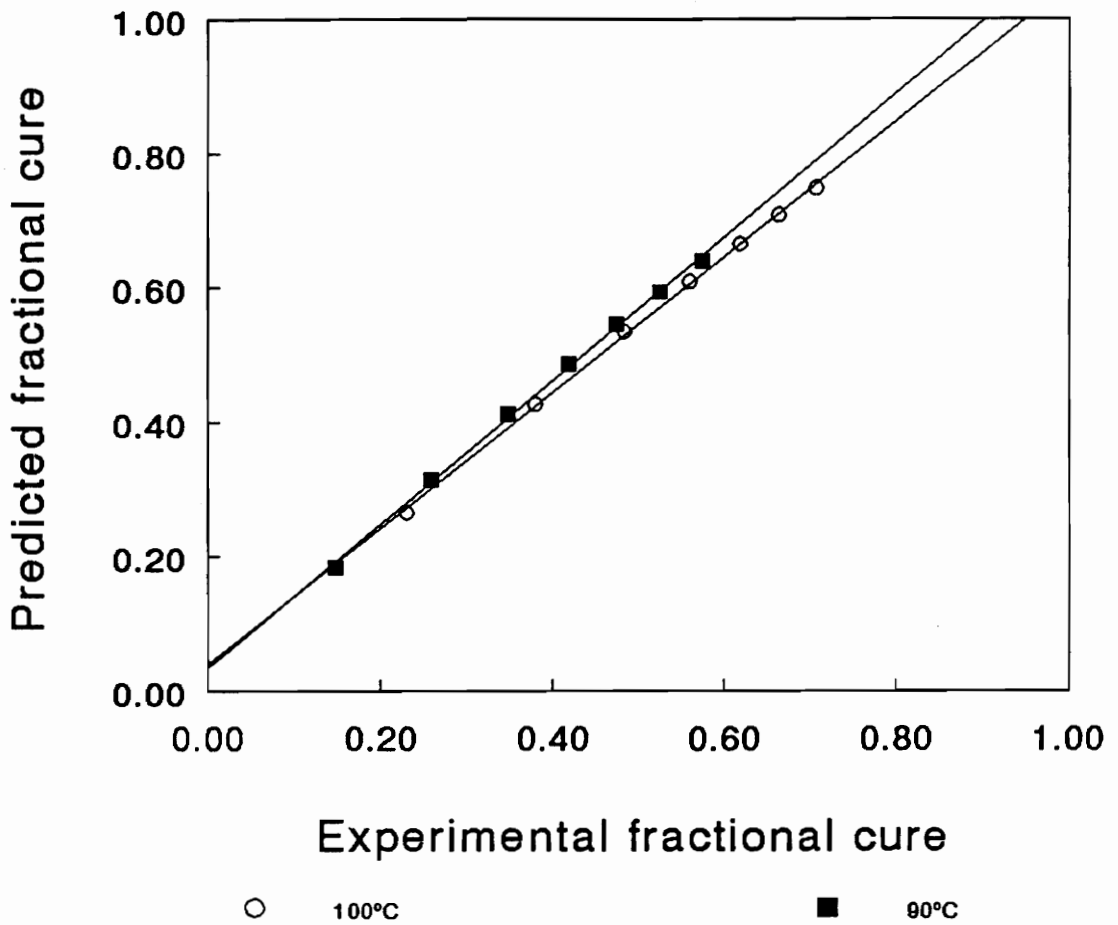


Figure 21. Evaluation of model equation and order of reaction of HPC-based polyurethanes. The solid line represents a curve fit to determine the correlation of the predicted fractional cure with experimental fractional cure.

are essentially constant for HPC- and HPL-based polyurethanes. This trend should suggest that the cure of these bio-based polymers is not entirely dependent on kinetic factors. Beyond vitrification, as seen in HPL-based polyurethanes, cure reactions become diffusion-controlled.

The results of the kinetic study analysis indicate that the model for cellulose react with isocyanate at a much lower rate, and attains a lower level of cure compared to that for lignin. The reaction of moisture (water) with isocyanate was very fast and no quantitative analysis could be done. This suggests that the order of reactivity with isocyanate takes the form

cellulose < lignin < moisture.

The application of HPL/MDI resin in bonding should offer an advantage over HPC/MDI resin in view of the long period required to achieve sufficient cure in the latter.

4.5 GLASS TRANSITION TEMPERATURE OF PARTIALLY CURED HPL-BASED POLYURETHANES

As demonstrated by Benci and Gillham (Figure 8), it is possible to construct a major portion of the gelation and vitrification curve by measuring the times to reach the first and second damping maximum in isothermal dynamic mechanical experiments.

This approach could not be successfully applied to the polymers studied. The isothermal traces of $\tan \delta$ or loss modulus do not show typical transitions as indication of vitrification and gelation (Figure 11 a & b). A quantitative approach, which takes advantage of the shiftability of T_g versus $\ln(\text{time})$ curves obtained from different cure temperatures was used to study the vitrification behavior of the HPL-based polymers. This approach, described in Section 2.3.3, has been applied successfully by Wissanrakkit and Gillham to develop a TTT diagram for epoxies.³⁶

The increase in T_g with time for five isothermal cure temperatures is presented for HPL-based polymers (Figure 22). All T_g versus $\ln(\text{time})$ curves were shifted horizontally along the $\ln(\text{time})$ axis, using appropriate shift factors calculated using equation 2.35 (Table 6) to an arbitrarily chosen reference temperature (80°C) to form a master curve.

The superposition demonstrates that before vitrification, defined as $T_g = T_c$, a smooth master curve is formed, but thereafter data points branch off from the master curve (Figure 23). Beyond vitrification, the cure reaction does not obey anymore an Arrhenius relationship of a kinetically controlled mechanism, but this becomes diffusion-controlled.³⁶ This accounts for the branch off of data points from the master curve.

The shift factors used in constructing the T_g versus $\ln(\text{time})$ master curve at 80°C were plotted against reciprocal cure temperature (Figure 24). The result can be correlated with a straight line ($R^2 = .998$), the slope of which yields an apparent

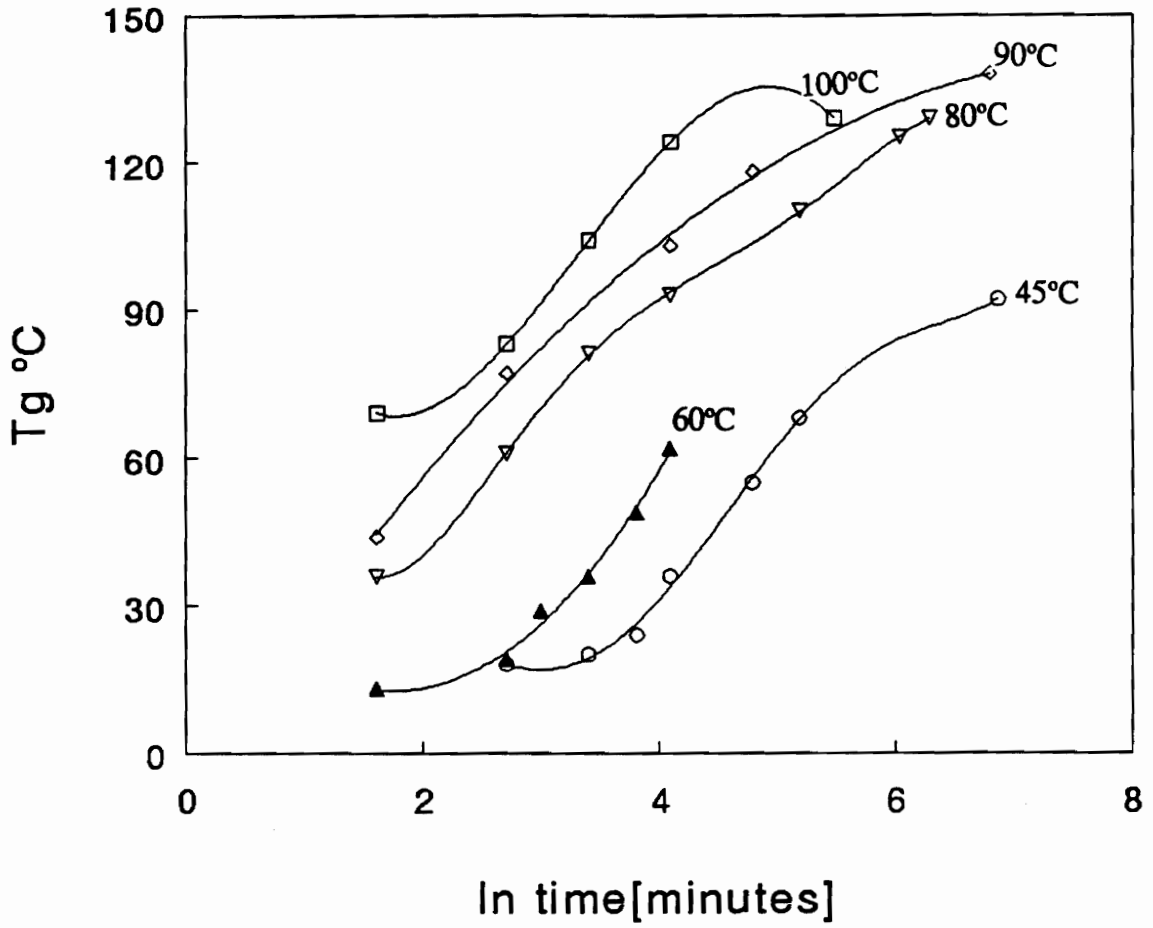


Figure 22. T_g of HPL-based polyurethanes versus time at various cure temperatures

Table 6. Shift factors for T_g superposition.

Temperature, °C	Shift factor
45	-2.47
60	-1.68
80	0
90	0.49
100	1.12

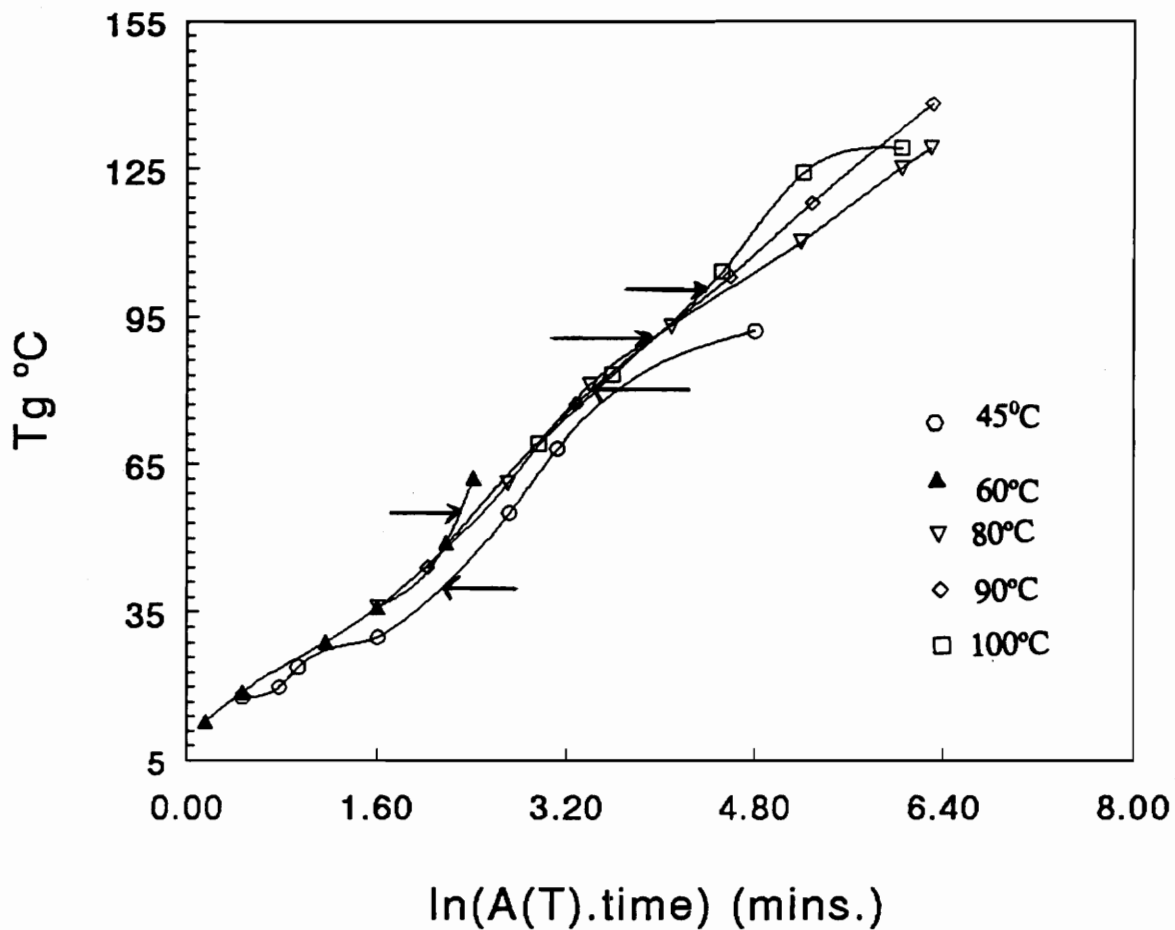


Figure 23. Superposition of the T_g vs $\ln(\text{time})$ data to form a master curve at an arbitrarily chosen temperature, 80°C, by shifting each curve in Figure 22 by a constant factor, $A(T) = \ln(t_{80}) - \ln(t_T)$ along the $\ln(\text{time})$ axis. Isothermal vitrification points, i.e. where $T_g = T_c$ at the various cure temperatures are indicated by arrows.

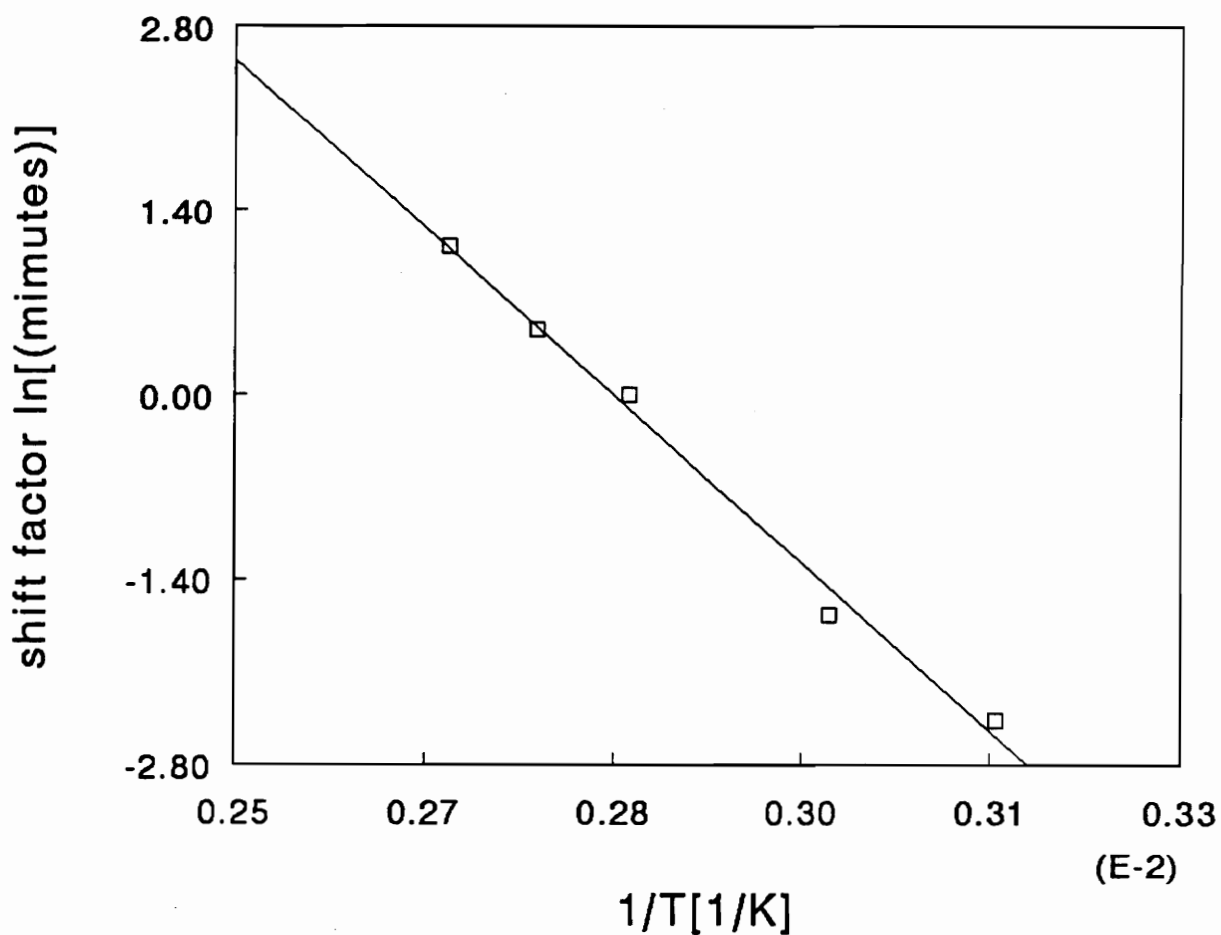


Figure 24. Arrhenius plot of shift factors, $A(T)$ used in constructing the master curves in Figures 23 and 24 versus $1/T(K)$. The activation energy for the reaction is determined from the slope of the resulting straight line.

activation energy for the cure reaction of HPL-based resins (equation 2.36), equal to 15.01 kcal/mol.

4.6 CONSTRUCTION OF VITRIFICATION CURVE IN A TTT DIAGRAM

Having defined $T_g = T_c$ as vitrification, equation 2.37 was recast as equation (4.2) to calculate the vitrification time, t_{vit} , at any cure temperature (T_c) based on the time (t_{ref}), necessary to reach a reference glass transition temperature, T_{gref} at a reference cure temperature, T_{cref} and the activation energy obtained.

$$\ln t_{vit} = \ln t_{ref} + \frac{E}{R} \left[\frac{1}{T_c} - \frac{1}{T_{cref}} \right] \quad (4.2)$$

The vitrification times are presented in a TTT cure diagram (Figure 25).

A similar analysis was attempted for HPC-based polymers with no success. The T_g for all isothermal cure times at any cure temperature were identical, and has been explained in the Section 4.2.

4.7 FRACTIONAL CURE VERSUS TIME SHIFTING

The T_g superposition approach was extended to variation of fractional cure with time, based on the fact that the equations governing the T_g superposition was

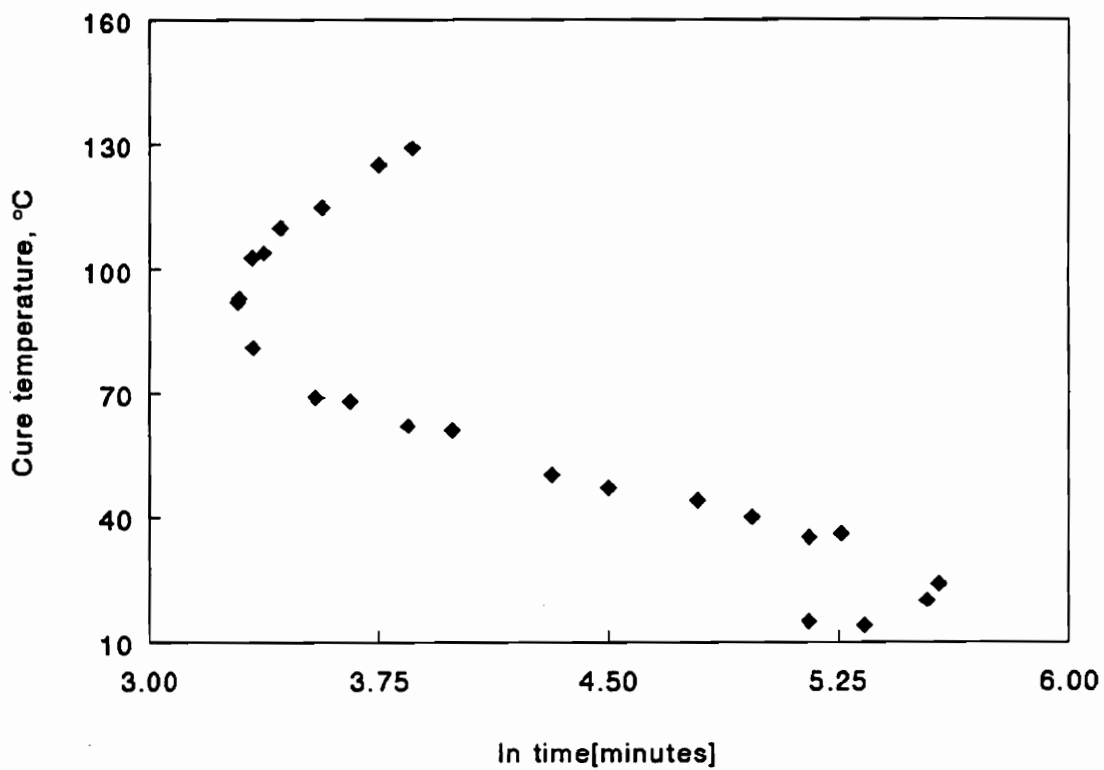


Figure 25. Calculated isothermal TTT diagram showing vitrification curve of HPL-based polyurethanes. The time to vitrification at the various cure temperatures were calculated from equation 4.2.

developed equating T_g to extent of conversion or fractional cure (equations 2.31 and 2.32).

Increase in fractional cure with time for five isothermal cure temperatures (from Figure 11) are presented for HPC-based polymers (Figure 26). These curves are shifted in a similar fashion, as in the case of T_g versus $\ln(\text{time})$ using appropriate shift factors, calculated from equation 2.35, to form a master curve at an arbitrarily chosen reference temperature, 120°C (Figure 27).

The apparent activation energy of the cure reaction was calculated, as 14.1 kcal/mol, from a plot of shift factor versus reciprocal temperature (Figure 28). The times to reach various levels of cure at different cure temperatures has been computed using equation (4.2), where T_g is replaced by fractional cure, to generate a series of iso-fractional cure curves (Figure 29).

This approach, involving degree of cure vs. time superposition has been used by Gillham and Wissarankit to calculate the apparent activation energy for epoxy resins. This approach is significant in studying the mechanical properties of a polymer at various levels of cure, and allows for a selection of cure schedules to achieve full cure.

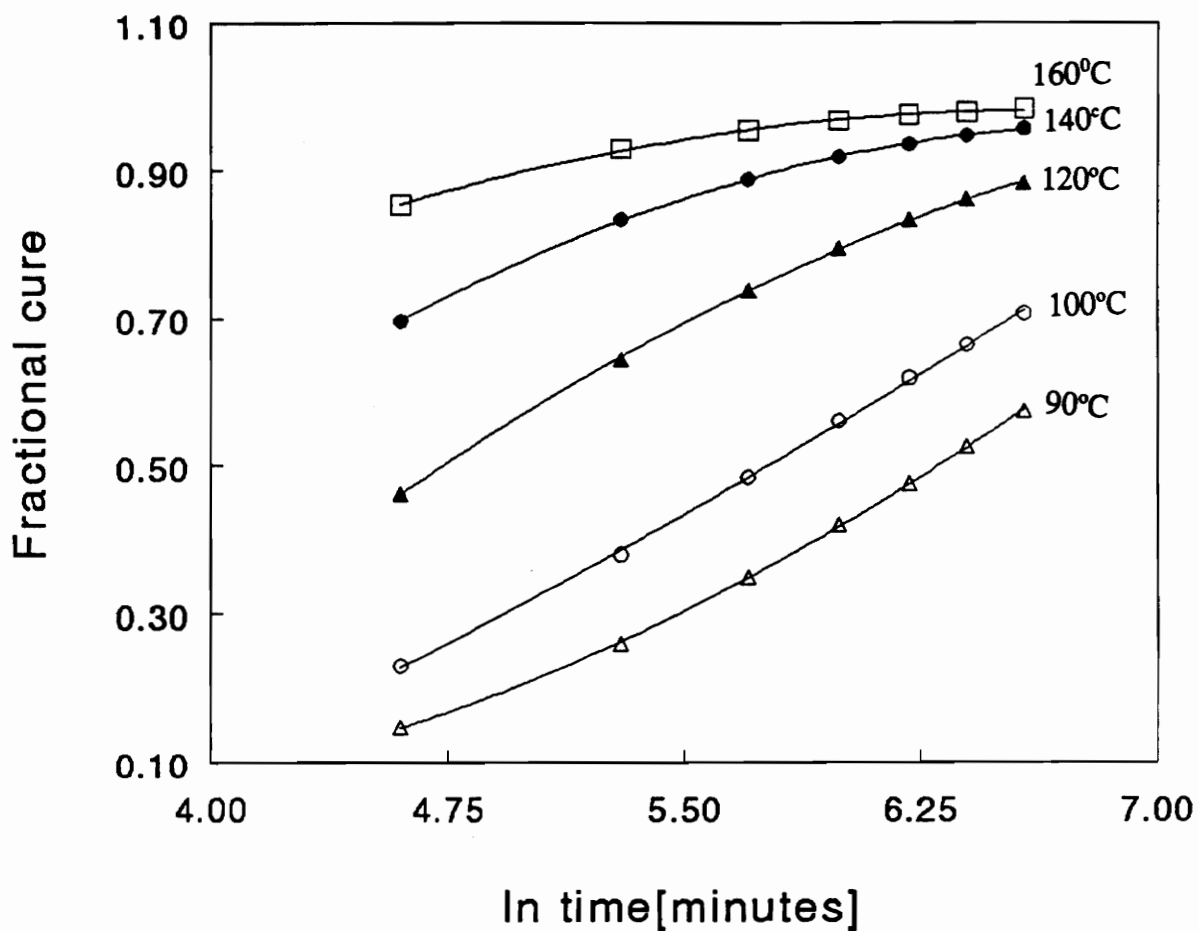


Figure 26. Fractional cure of HPC-based polyurethanes versus time at various temperatures.

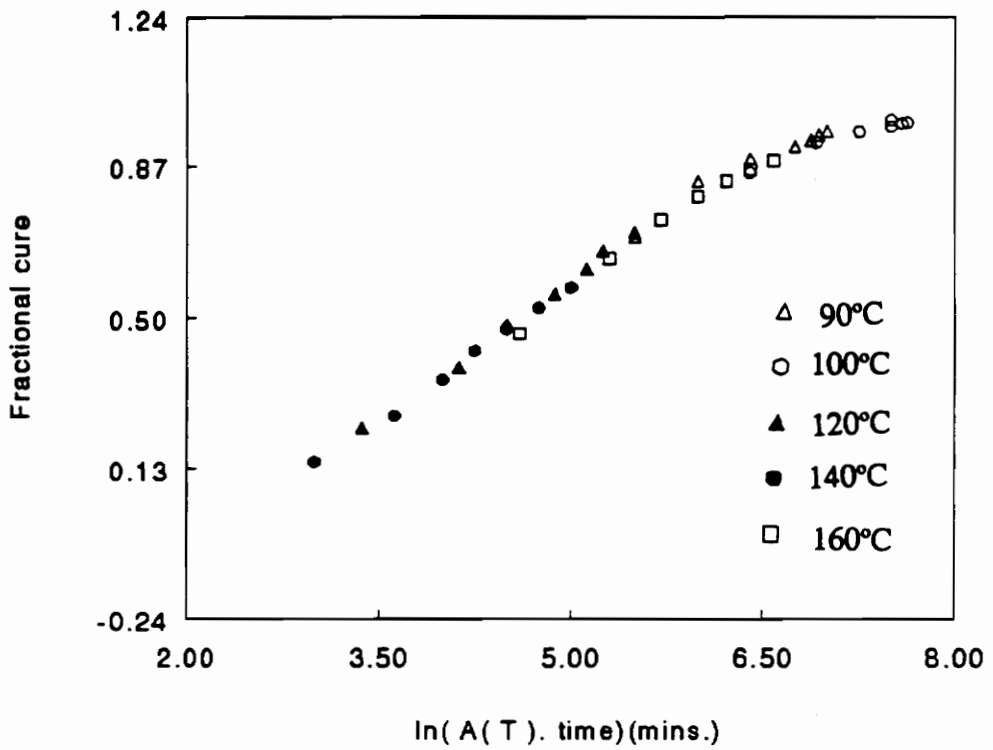


Figure 27. Superposition of fractional cure vs $\ln(\text{time})$ data to form a master curve at an arbitrarily chosen temperature, 120°C , by shifting each curve in Figure 26 by a constant factor $A(T) = \ln(t_{120}) - \ln(t_T)$ along the $\ln(\text{time})$ axis.

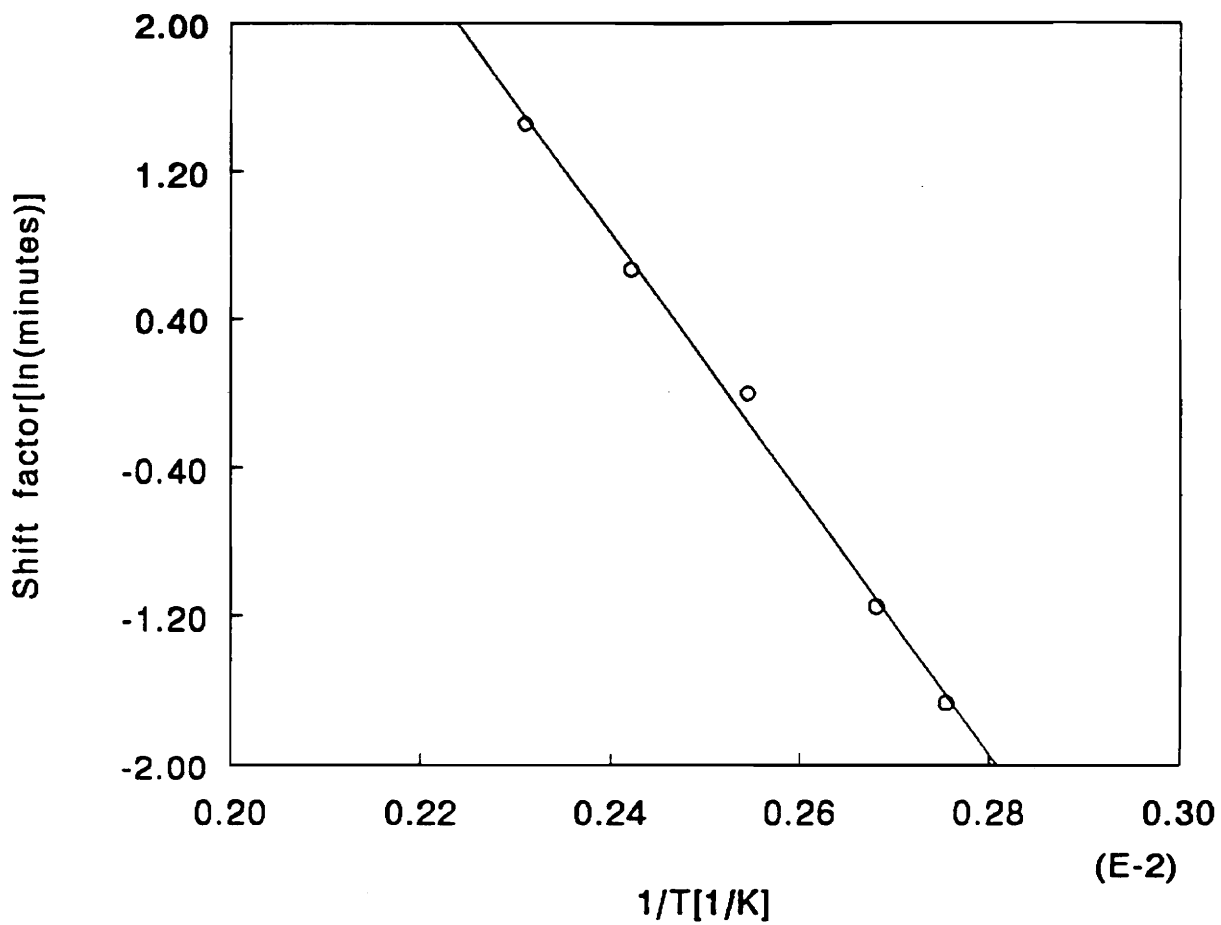


Figure 28. Arrhenius plot of shift factors $A(T)$, used in constructing the fractional cure master curve at 120°C versus reciprocal temperature.

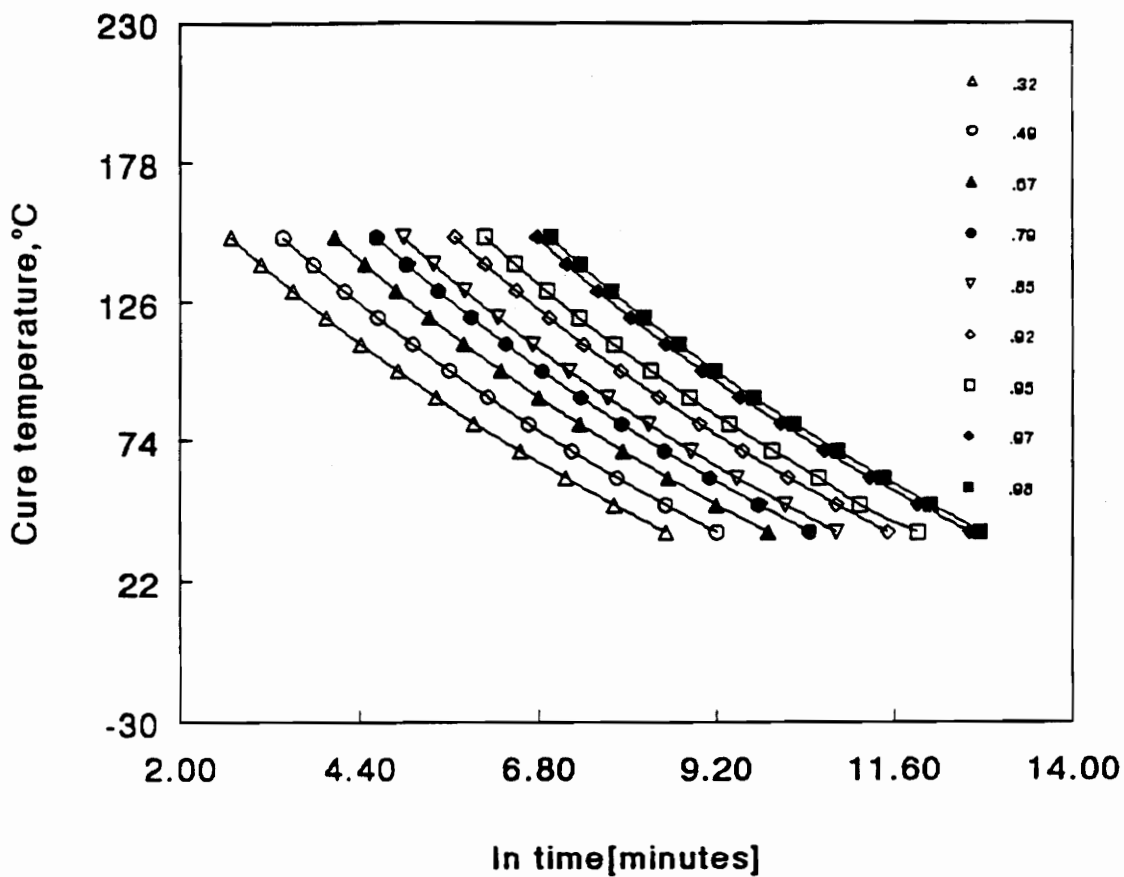


Figure 29. Iso-fractional cure profile of HPC-based polymers. The various lines represent different levels of cure, i.e. fractional cure, and have been generated using equation 4.2, where T_g is replaced by fractional cure.

4.8 EFFECT OF RESIN STOICHIOMETRY ON NETWORK FORMATION

Variation of resin stoichiometry, i.e. ratio of NCO to OH, and its effect on network parameters such as T_g and damping characteristics was investigated in this section. The T_g obtained at various ratios, for samples cured at 90°C for 12 hours, is presented (Figure 30) where the T_g is plotted against NCO:OH. T_g shows a positive linear relationship with increasing ratio.

To quantify the variation of energy barriers to segmental motion in the network at various ratios, at the glass transition temperature, the activation energies were determined from multi-frequency dynamic mechanical analysis of fully-cured samples (Figure 31). The activation energies have been obtained from a $\ln(\text{frequency})$ versus T_g^{-1} plot (Figure 32) and are compiled in Table 7. There is an increase of the activation energy with increasing NCO to OH ratio (see Figure 30); however, the increase lies in a very narrow range, presumably due to the narrow range of ratios studied. Increasing NCO to OH ratio is reported to increase crosslinking^{38,46}. The greater the degree of crosslinking, the more important is the hinderance to the cooperative relaxation process associated with the glass transition temperature. The ultimate effect is increased activation energy barrier, and appearance of the relaxation process at higher temperatures. Therefore, the rise of T_g and activation energy with increasing NCO to OH ratio is as expected.

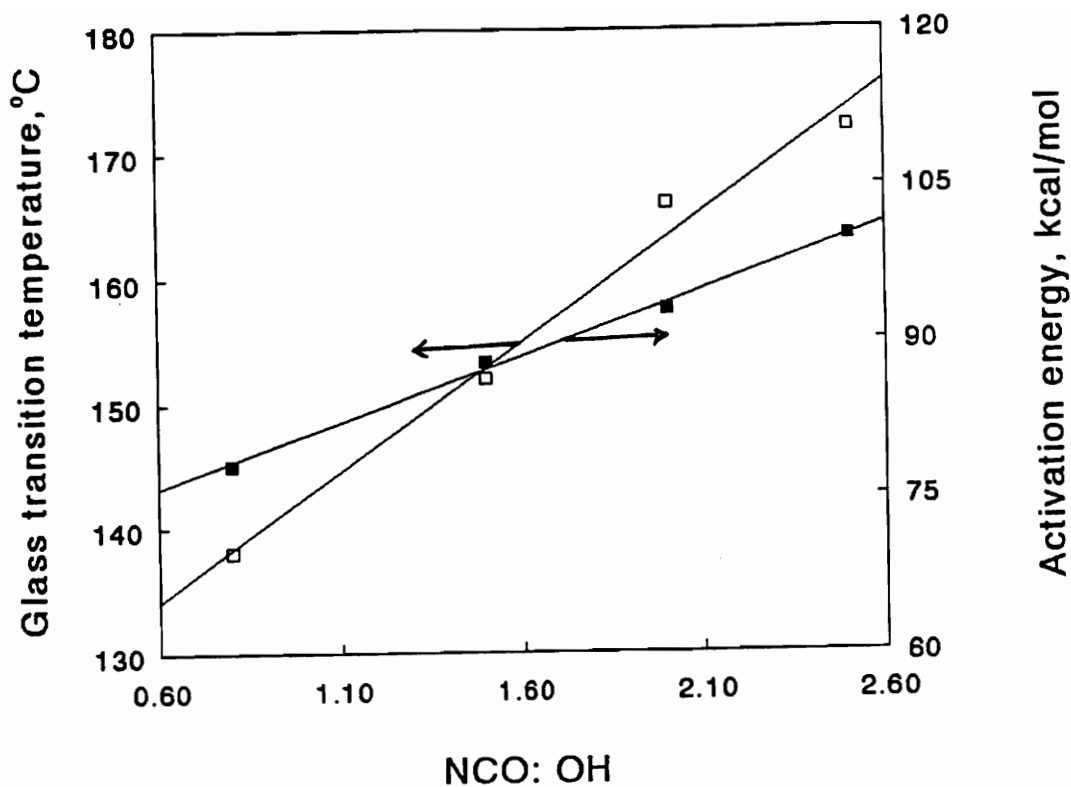


Figure 30. The variation of T_g and its activation energy derived from an Arrhenius plot of \ln frequency versus T_g , with resin stoichiometry. The system studied was HPL-based polyurethanes at various stoichiometries. Both T_g and the corresponding activation energy increase with increasing resin stoichiometry.

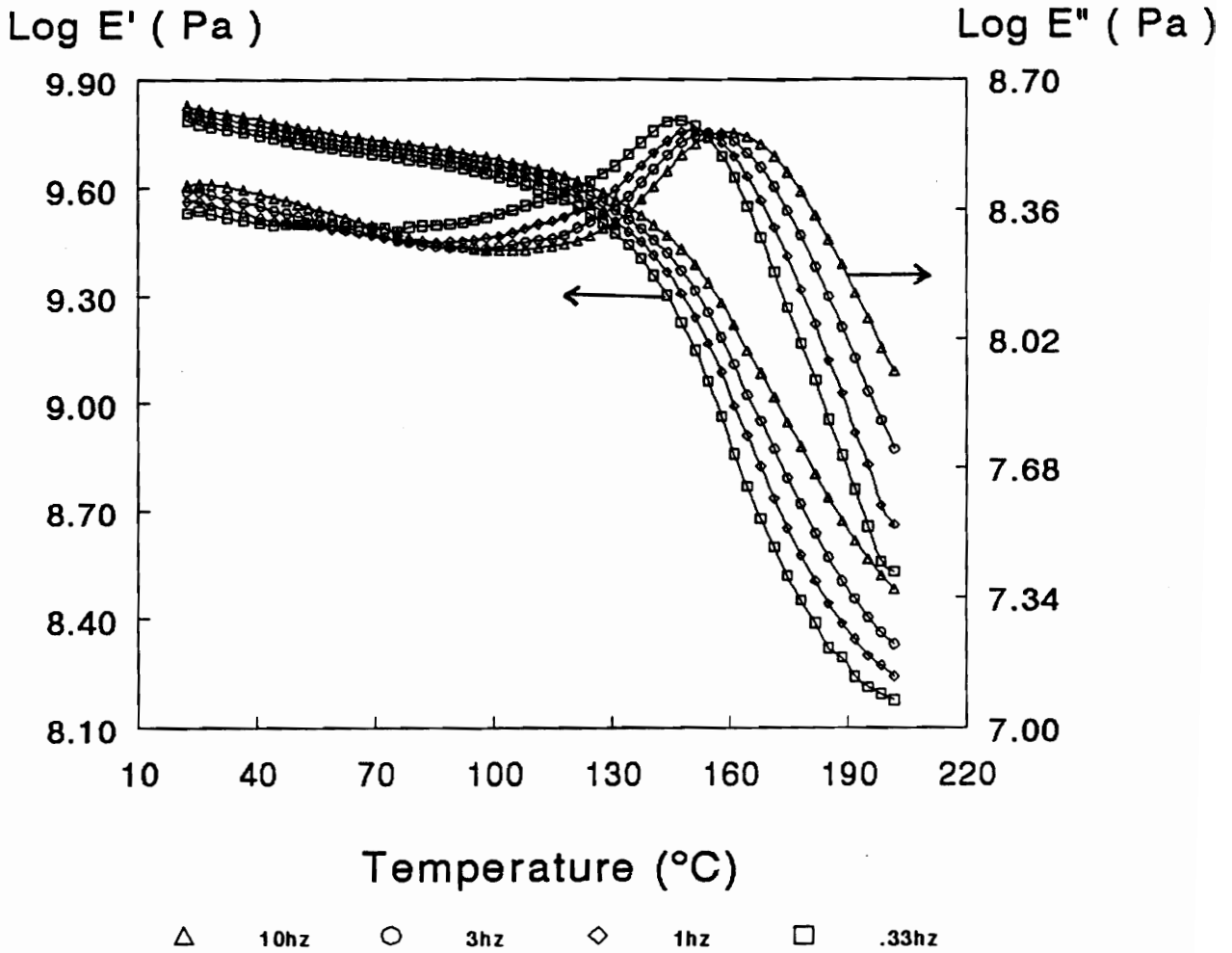


Figure 31. DMTA spectra of HPL-based polymers showing the effect of frequency on T_g . This represents the multifrequency DMTA spectrum of NCO:OH of 1.5.

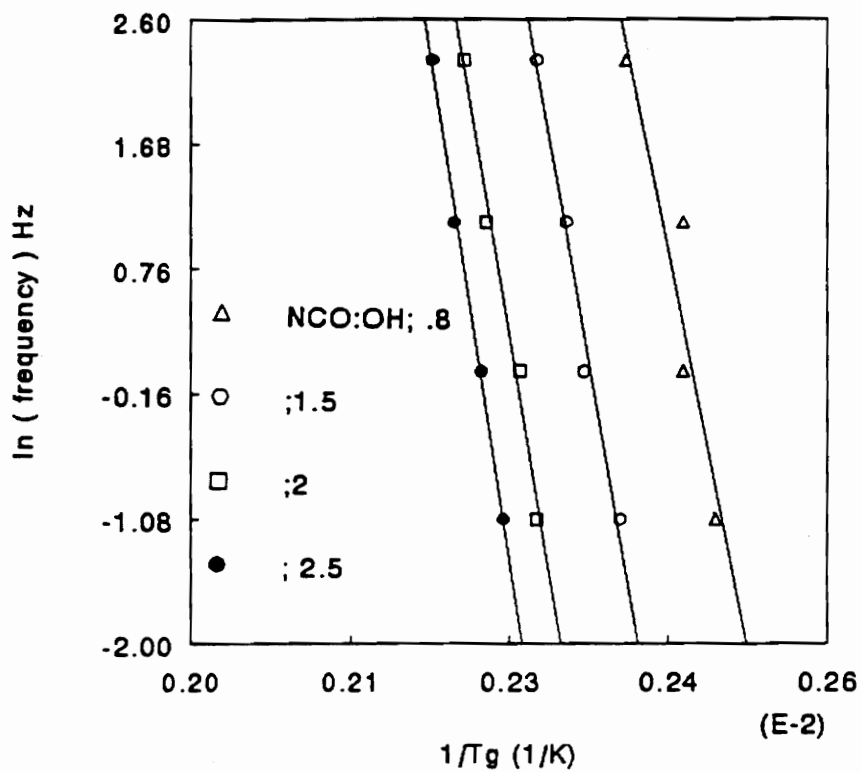


Figure 32. Arrhenius plot of (frequency) versus T_g for the determination of the activation energy of T_g of HPL-based polyurethanes at various resin stoichiometries.

Table 7. Activation energies of T_g at various resin stoichiometries.

E_A (kcal/mol)	NCO:OH
78	0.8
88	1.5
93	2.0
100	2.5

The peak width and transition amplitude of the loss modulus increased with increasing and decreasing NCO to OH ratio, respectively (Figure 33).

The peak width of transitions has implications on the energy dissipation or damping performance of a polymer. If the transition is narrow, the optimum-use temperature range is also narrow and slight changes in temperature result in loss of damping characteristics. A material with a broad transition range could be used over a wider range of temperatures without losing damping capability.^{2,13} Based on this analogy, it becomes obvious that increasing NCO:OH produces polyurethanes capable of retaining damping characteristics over a wider range of temperatures. Very often a necessary trade-off of increasing the temperature or frequency range of damping or transitions is the reduction of the $\tan \delta$ amplitude, i.e., lower E'' values and higher E' components.² Thus, the decreased amplitude at higher NCO:OH ratio is as expected.

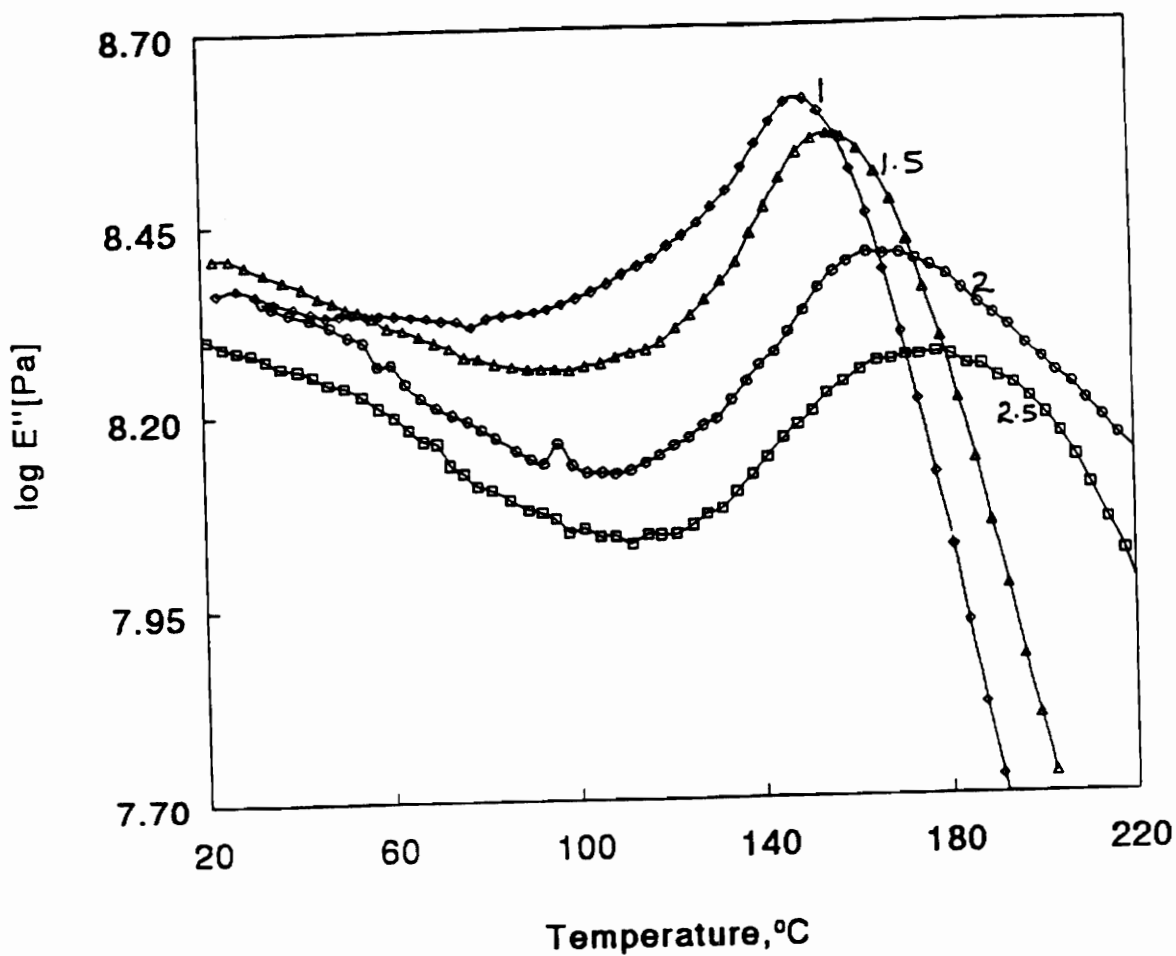


Figure 33. Change of damping characteristics in HPL-based polymers with NCO:OH. There is a progressive increase in the breadth of the damping peak with increasing resin stoichiometry. The opposite is true of the height of the damping peak.

CHAPTER 5

5.0 CONCLUSIONS

Concluding, it can be said about the cure reaction of HPC and HPL with MDI that:

- It is possible to obtain isothermal and dynamic scan kinetic cure parameters for HPC and only dynamic scan parameters for HPL by DMTA.
- HPC and HPL react with MDI following n^{th} order kinetics, with an order of reaction 1.8 (≈ 2) and an apparent activation energy of 12.9 - 14.78 kcal/mol.
- These values of the activation energy are in the same range as those reported for other polyurethanes.
- HPL lends itself more readily to crosslinking than HPC. Both react with isocyanate (MDI) at a reduced rate compared to a synthetic polyol; caprolactone triol.
- HPL-based polyurethanes are more thermally stable than HPC-based ones (see Figures 9 and 10).
- Isothermal $\tan \delta$ or loss moduli did not permit the identification of gelation and vitrification based on damping maxima, as it is possible for most thermosetting polymers.

- Master curves of T_g versus cure time for isothermal cure temperatures, 45°C - 100°C, could be constructed for HPL-based polyurethanes, and the activation energy calculated from shift factor ($A(T)$) versus T^{-1} plot. This approach did not work for HPC-based polymers.
- It was possible to construct vitrification curve in the form of a TTT cure diagram, based on the knowledge of activation energy and cure times at a reference temperature to reach a given glass transition temperature.
- A master curve of fractional cure versus cure times for isothermal cure temperatures ranging from 80°C to 160°C, could be constructed for HPC-based polymers, and the activation energy calculated from shift factor ($A(T)$) versus T^{-1} plot. The activation energy compared favorably with that obtained in the kinetic analysis.
- The T_g of HPL-based polymers, and the corresponding activation energies increase with increasing resin stoichiometry (NCO:OH).
- Damping characteristics over a wide temperature range is improved at high resin stoichiometry.
- The study also reveals that the reaction of water with isocyanate and the reaction of HPL and HPC with isocyanate in solution follow the order: water > HPL > HPC. This trend might be similar to the relative reactivity of cellulose, lignin, and moisture with isocyanate during wood bonding.

In terms of practical significance, it could be concluded that

- HPC-based polyurethanes offer an advantage over their HPL-based counterparts, where retention of stiffness is desired, though the former takes a longer time to achieve sufficient cure. This is only true of temperatures below 230°. Beyond 230°, HPC-based polyurethanes are not thermally stable.
- HPL-based polyurethanes are more desirable for damping applications than are HPC-based polyurethanes.
- It is essential to use high isocyanate to hydroxyl ratios in order to derive HPL-based polyurethanes with good damping behavior over a wider temperature range.
- Lignocellulosic-based polyurethane resins offer an advantage over caprolactone triol-based in applications where sufficient spread and/or flow is necessary. The latter might gel before sufficient spread of resin and assembly.

REFERENCES

1. Adhesive bonding of wood and other structural materials. Vol. III Forest Service, USDA Series, 1981.
2. Aklonis, J. J. and MacKnight, W. J. Introduction to viscoelasticity. Wiley-Interscience, NY. 1983.
3. Aronhime, M. T. and Gillham, J. K. J. Coat Tech. 56(718) 1984 J. Appl. Polym. Sci. 35, 29, 1984, 29, 2017 (1984)
4. Bauer, D. R. and Dickie, R. A., Ind. Eng. Chem. Prod. Res. Dec. 25, (1986).
5. Billmeyer, F. Textbook of Polymer Science, Wiley, NY, 1984.
6. Buist, J. M. and Gudgeon, Advances in Polyurethanes technology. John Wiley and Sons, NY, 1968.
7. Chambon, F. and Winter, H. H. J. Rheol. 30, 367 (1986).
8. Chan, L. C., Kinloch, A. J. ACS 208, 235 (1984).
9. Chan, L. C., et al. J. Appl. Polym. Sci. 29(3307) 1984.
10. Connolly, M. and Tobias, B. American Lab. (1992).
11. Edith Turi. Thermal Characterization of Polymeric Materials, Academic Press, NY. 1981.
12. Feger, et al. Macromolecules, 17(9) 1984.
13. Ferry, J. D. Viscoelastic properties of polymers. J. Wiley & Sons, NY. 1983.
14. Follensbee, R. A. J. Polym. Sci. 43, 235-50 (1991).
15. Flory, P. J. Principles of Polymer Chemistry.
16. Gillham, J. K. Thermomechanical properties of polymers by TBA, ASCE Journal. Vol. 20, 6, 1974, in Developments in Polymer Characterisation-3, J. V. Dawkins Ed. Applied Science, London 1982, in Developments in Structural Adhesives, edited by A. J. Konloch.

17. Gillham, J. K. and Enns, J. B. *J. Appl. Polym. Sci.* 28, 2567, 2831, 1983, ACS Symp. Series 197, 329 (1982).
18. Gillham, J. K. and Benic, J. *Poly. Sci. Symposium No. 46*, 279-289 (1974).
19. Hofmann, K. Ph.D. dissertation, Virginia Tech. 1991.
20. Hofmann, K and Glasser, W. G. *Proceedings of the 17th NATAS Conference. Vol. 1, 1989, Thermochemica Acta, No. 166*, 169-184 (1990).
21. K. C. Frisch, in *Polyurethane Technology*, PF Bruins, Ed., Wiley Interscience, NY, 1969.
22. Kendell, D.N. *Appl. Infrared Spectroscopy*. Reinhold Publishing Corp. London, 1966.
23. Kelley, S. S. and Glasser, W. G. *J. Wood Chem. & Tech.* 8(3):341-59 (1988).
24. Kelley, et al. *J. Mat. Science.* 617-624 (1987), *J. Appl. Sci.* 37, 29961 (1989).
25. Kontsky and Ebewe. *Chemistry and properties of cross-linked polymers*, Academic Press, NY. 1977.
26. Knop and Scheib. *Chemistry and applications of phenolic resins*. Springer-Verlag, NY. 1979.
27. Macosko, C. W. and Miller, D. R. *Macromolecules*, 9, 199 (1976).
28. Meyer and Wennesleimer, *Holzforchung*. 1989.
29. Mussati, G. F. Univ. of Minnesota, Ph.D. dissertation. 1975.
30. Nielson, L. F. *Mechanical properties of Polymers*. Van Nostrand, Reinhold Co. NY, 1962.
31. Niranjan, M. P. et al. *Proceedings of the 17th NATAS Conference. Vol. 1 (1989)*.
32. Owusu, O. and Martin, G. C. *Polym. Eng. Sci.* 32, 8, 535-41. 1992.
33. Petrovic et al. *J. Appl. Polym. Sci.* 29, 1031-1040 (1984).

34. Provder, T. J. *Coat. Tech.* 61, 770, 1989.
35. *Polymer characterization: spectroscopic, chromatographic, and physical instrumental methods.* Ed. Craver, C. D. ACS 208, 21-94 (1981).
36. *Polymer characterization: physical property, spectroscopic, and chromatographic methods.* Ed. Craver, C. D. and Provder, T. ACS 227, 143-166 (1988).
37. Roboredo, M. M. and Williams, R. J. J. *Polym. Journal* 15 9-14 (1983).
38. Rials, T. G. Ph.D. dissertation, Virginia Tech (1985).
39. Rials, T. G. and Glasser, W. G. *J. Wood Chem. & Tech.* 4(3):331-45, 1985.
40. Richter, E. B. and Macosko, C. W., *Polym. Eng. Sci.* 18, 1012. 1978.
41. Stockmayer, W. H. *J. Polym. Sci.* 9, 69 (1952).
42. Tonogan and Sakaguchi. *J. Appl. Polym. Sci.* 22 (1978).
43. *Theory of Operation of Dupont DMA: Operators' manuals.* DuPont Corporation 1985.
44. *The Perkin Elmer Model DSC-2: Operators' manuals.* Perkin Elmer Corporation 1985.
45. Young and Kopf. *Tappi* 64(4) 1984.
46. Yoshida, H. *J. Appl Polym. Sci.* 34, 1187-98 (1987).
47. *Wood Adhesives: Chemistry and Technology*, ed. Pizzi, A. Marcel. Dekker, Inc. 289-316 (1983).
48. Williams, D. J. *Polym. Eng. and Science*, Prentice-Hall, NY, 1971.
49. Wright, P. and Cummings, A.P. C., *Solid Polyurethane elastomers.* McClaren and Sons, London. 1969.
50. Zumbum, M. A. Ph.D. dissertation, Virginia Tech, 1991.

VITA

The author, son of J.S.A. Toffey and Ekye Menwube, was born in October 1965 in Kumasi, Ghana. He earned a bachelor's degree in Natural Resources Management in 1989 at the University of Science and Technology, Kumasi, Ghana. After completion of the Ghanaian mandatory students service, Ackah enrolled in Virginia Tech in August 1991. Ackah will receive his master's degree in December 1993.

A handwritten signature in black ink, appearing to read 'Ackah', with a stylized flourish at the end.